Acta Mech 229, 1869–1892 (2018)
https://doi.org/10.1007/s00707-017-2054-6

ORIGINAL PAPER

Pramod Kumar Yadav · Ashish Tiwari · Priyanka Singh

Hydrodynamic permeability of a membrane built up by spheroidal particles covered by porous layer

Received: 5 July 2017 / Revised: 10 September 2017 / Published online: 23 December 2017

Abstract This paper concerns the motion of a viscous steady incompressible fluid through a membrane, where the membrane is built up by impermeable spheroidal particles covered by a porous layer. In this work, we discuss the hydrodynamic permeability of a membrane built up by spheroidal particles. Cell model technique has been used to find the hydrodynamic permeability of the membrane. The emphasis is placed on the hydrodynamic permeability of the membrane and its controlling parameters like the permeability of the porous medium, particle volume fraction, deformation parameters, stress jump coefficient. The dependency of the hydrodynamic permeability of the membrane on the above controlling parameters is discussed graphically. Some previous results for hydrodynamic permeability and drag force are verified.

1 Introduction

Flow through a porous medium made of a swarm of particles has always been a topic of immense interest due to its numerous applications in various fields of science and engineering, such as ground water flow, flow through sand beds, petroleum reservoirs, flow through biological tissues and filtration processes. However, modelling and formulation of such a complex fluid dynamical system are a big challenge to mathematicians so as to arrive at a satisfactory approximation of the system at macroscopic level, which includes employing the Darcy [1] or the Brinkman equation [2] for the flow through the porous region and the Stokes equation [3] in the free flow region with appropriate and physically realistic boundary conditions for a suitable approximation of the system.

The Darcy equation is more suitable for a medium with low permeability and inhomogeneous porosity, as for a higher-permeable region the equation yields a contradictory result (higher flow at zero pressure difference). To overcome this drawback, Brinkman suggested a modification in Darcy's equation by adding a term for viscous forces using different viscosities in the porous medium due to the porosity effect, and it worked well for both low- and high-permeable regions. However, for inhomogeneous porous media, the formulation has some limitations near the boundary as suggested by Veerapanneni [4].

The flow of a viscous fluid through a random assemblage of particles is a challenging task due to the complexity involved in its modelling and formulation as we intend to have complete information about the

P. K. Yadav (✉)
Department of Mathematics, Motilal Nehru National Institute of Technology Allahabad, Allahabad 211004, India
E-mail: pramod547@gmail.com

A. Tiwari
Department of Mathematics, Birla Institute of Technology and Science, Pilani, Rajasthan 333031, India
E-mail: ast79.ashish@gmail.com

P. Singh
Department of Mathematics, National Institute of Technology Patna, Patna 800005, India
E-mail: rosaindica2k@gmail.com

flow field and other relevant quantities such as drag near all the particles. In order to overcome this problem, it was suggested that instead of going for flow information near each particle, the attempt should be made to compute the same near one particle confined in a hypothetical cell surface and appropriate and physically realistic boundary conditions should be imposed on the concerned particle to include the effect of neighbouring particles on the particle confined within the hypothetical cell. This approach is known as cell model technique. Uchida [5] made the first attempt in this direction by taking a spherical particle covered in a cubical cell. Although the cubical cell is space filling, differences in the inner and outer geometry made the problem mathematically very complicated. In order to overcome this problem, Happel [6,7] took both the particle and cell surface of the same geometry and employed the condition of vanishing shear stress at the cell to take into account the zero friction exerted by neighbouring particles on the particle concerned. Kuwabara [8] followed the same approach with vanishing rotation at the cell surface and observed the exchange of mechanical energy between fluid envelope and the environment. Mehta–Morse [9]/Cunningham [10] used the uniform velocity condition on the fluid envelope confining the concerned particle, which takes into account the homogeneity of flow at the fluid envelope. Kvashnin [11] used the condition that the tangential component of velocity attains its extreme value at the cell surface along the radial direction, signifying symmetry in the flow. There are many authors who applied the above formulations in various physical models. Yadav et al. [12] evaluated the hydrodynamic permeability of a swarm of solid spherical particles with a porous layer for all four cell model formulations using a stress jump at the fluid–porous interface. Deo et al. [13] gave a detailed review of work done in this area along with a comparative analysis of all the four formulations for a swarm of cylindrical particles.

In addition to the above, there are many more papers on flow through a swarm of spherical and cylindrical particles, but the geometry of the particles may be more complicated than spherical or cylindrical shapes. The Stokes stream function formulation $E^4\psi = 0$ (where E^4 is a well-known operator [14]) is relatively simple in Cartesian, cylindrical or spherical coordinate systems due to the separable nature of the Stokes stream function in all of them. However, there are several complex geometries where this property does not hold for the stream function formulation equation governing axi-symmetric Stokes flow. In the quest for modelling flows through an assemblage of particles with complex geometry, many authors made attempts to look for Stokes' stream function solutions in other coordinate systems and the spheroidal coordinate system is one of them. The non-separability of $E^4\psi = 0$ in a spheroidal coordinate system hampers the development of modelling the flows through an assemblage of spheroidal particles. Despite these complexities, the flow past spheroidal or ellipsoidal bodies attracted researchers in the nineteenth century. Oberbeck [15] analytically investigated the creeping flow due to steady translatory motion of an ellipsoid embedded in an unbounded fluid medium by solving the equation in a Cartesian coordinate system. Sampson [16] analysed the Stokes flow past a spheroid embedded in an unbounded fluid medium and translating around its main axis. The advantage of Sampson's work was use of spheroidal coordinate systems in the analysis. Axi-symmetric Stokes' flow past a spheroid in an unbounded fluid and translating around its main axis was analytically studied in spheroidal coordinates by Payne and Pell [17]. They also obtained the solution for their problem by a suitable transformation of Oberbeck's solution for an ellipsoid leading to a change of coordinates. Happel and Brenner [14] also analytically solved the creeping flow problem past a spheroid in spheroidal coordinates. Acrivos and Taylor [18] studied flow past an arbitrary particle and obtained the expression for drag force for a slightly but arbitrarily deformed sphere. Epstein and Masliyah [19] investigated the Stokes' flow through swarm of oblate spheroids and elliptical cylinders. They observed that for low aspect ratios and high volumetric particle concentrations, there is significant deviation in Kozeny constant for axi-symmetric flow past both types of particles. Although this analysis was based on numerical solutions only. Ramkissoon [20] studied symmetric slow flow past a fluid spheroidal particle (slightly deformed from a sphere) in an unbounded medium and also covered the flow past an oblate spheroidal particle as a special case. It was also observed that with equal volume of fluid sphere and oblate fluid spheroid, the fluid sphere will experience less resistance. Palaniappan [21] analysed creeping flow of an incompressible viscous fluid past a deformed sphere (slightly deformed from spherical shape) with slip-stick boundary conditions up to a first-order approximation of the deformation parameter by obtaining the stream function for the flow field in terms of the Gegenbauer function and deduced the dependence of the functional form of the hydrodynamic drag on the eccentricity of the spheroid, and unlike the previous result [20], the drag on the spheroid need not be linear due to a change in boundary conditions. He observed that the slip-stick boundary condition parameter significantly affects the drag force experienced by the deformed sphere and also found a relatively smaller drag on the deformed sphere in comparison to the drag on a slightly oblate spheroid. Dassios et al. [22] used the semi-separable nature of the stream function satisfying Stokes' equation in spheroidal coordinates to get the analytical solution of axi-symmetric creeping flow past an oblate/prolate spheroid in a spheroidal cell by

deriving a complete set of generalized eigenfunctions. Dassios et al. [23] used the Stokes stream function obtained for a spheroidal coordinate system in [22] to analyse the spheroid-in-cell problem using Happel and Kuwabara boundary conditions and concluded the superiority of the Happel condition over the Kuwabara condition due to smaller loss of mechanical energy. Burganos et al. [24] discussed the convergence of the semi-separable expansion of the Stokes stream function up to first order and observed a high level of accuracy for the axis ratio lying in the range $\left[\frac{1}{5}, 5\right]$ and solid volume fraction lying in the range of [0, 0.3]. Ramkissoon [25] analytically studied the slip flow past an approximate spheroid and concluded that among sphere and spheroid (equatorial radius of the spheroid the same as that of the sphere), the oblate spheroid experiences a relatively smaller drag than the sphere and the proportion to which it reduces remains the same for both no-slip and perfect-slip cases. Zlatanovski [26] investigated creeping flow past a porous prolate spheroidal particle using eigenvalues and eigenfunctions of the stream function for the porous region and graphically discussed the effect of focal distance and permeability parameter on drag force and stream lines. Dutta and Deo [27] evaluated the drag force experienced by particles of cylindrical, spherical, deformed sphere and oblate spheroid geometry by considering Stokes flow past a swarm of particles with slip and Kuwabara boundary conditions. They used the stream function formulation up to first order of the deformation parameter to obtain the stream function. Srinivasacharya [28] studied the effect of permeability on the drag force experienced by a porous approximate sphere by using the Brinkman and Stokes stream function formulation for flow in a porous region and a clear fluid region, respectively, and also deduced the results for flow past a spherical body as a special case (deformation parameter tends to zero). Deo [29] evaluated the drag force experienced by each deformed porous oblate spheroidal particle in a cell using the Happel boundary condition. Deo and Gupta [30] investigated the Stokes flow past a swarm of porous approximately spheroidal particles using the Kuwabara boundary condition at the cell surface. They studied the dependence of the drag force on the permeability of the medium for different values of the deformation parameters for a spheroid in an unbounded medium and also analysed the effect of volume fraction of drag force for a spheroid in a cell case. Yadav and Deo [31] investigated the creeping flow past a porous spheroid embedded in another porous medium and observed the effect of the permeability parameter for one medium on shear stress and drag experienced by the particle for different porosities and different values of permeability parameters for the other medium. Yadav et al. [32] evaluated the permeability of a swarm of deformed porous spheroidal particles using the cell model technique and graphically discussed the behaviour of drag force and hydrodynamic permeability with volume fraction, permeability parameter, deformation parameter, etc.

The present paper concerns the creeping flow past a swarm of solid spheroidal particles covered with porous layers with a particle in cell approach. All four cell model boundary conditions have been employed on the hypothetical cell surface, and the effect of volume fraction and other parameters on the drag force has been studied.

2 Mathematical formulation of the problem

In the present model, we have taken a membrane which consists of identical deformed spheroid particles covered by the porous layer. In this model, we are assuming that the axis of each deformed spheroidal particle in the membrane is parallel and all spheroidal particles are identical. Due to the above assumption, the considered membrane will become homogeneous and isotropic. Here, we assume that the steady, axi-symmetric, viscous, incompressible fluid is flowing through the membrane with uniform velocity $\tilde{\mathbf{U}}$ ($|\tilde{\mathbf{U}}| = \tilde{U}$) directed along the positive z axis and the porous deformed spheroid particles are stationary. To find the hydrodynamic permeability of the membrane built up by the above identical deformed spheroid particles, we select a single particle from the swarm and assume that it is confined within a hypothetical cell whose shape is the same as the selected deformed spheroidal particle (Fig. 1).

This type of problem arises when the shape of the swarm of porous sphere will change because of the applied force from the fluid flowing through the swarm of porous spherical particles. Let the surface of an inner impermeable spheroid named as S_{Im} be

$$\tilde{r} = \tilde{a}(1 + \beta_m G_m(\zeta)), \qquad \tilde{a} = d_1(1 - \varepsilon), \tag{1}$$

and the surface of a porous spheroid named as S_P be

$$\tilde{r} = \tilde{b}(1 + \beta_m G_m(\zeta)), \quad \tilde{b} = d_2(1 - \varepsilon). \tag{2}$$

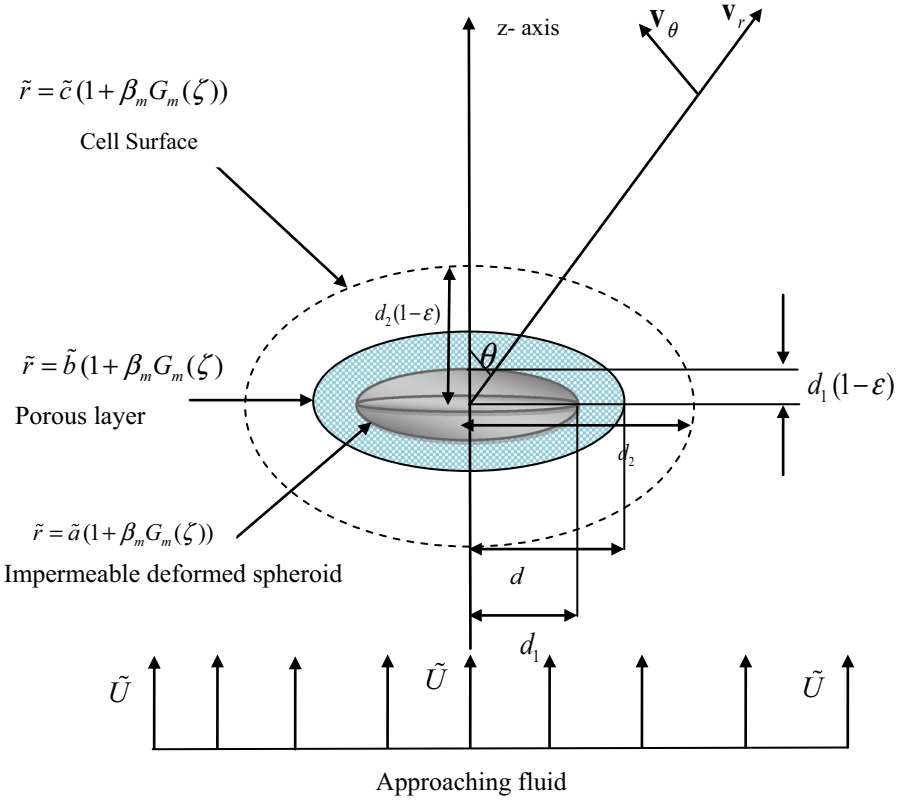

Fig. 1 Physical model and coordinate system of the problem

The equation of the outer cell surface, i.e. the hypothetical surface S_H, is

$$\tilde{r} = \tilde{c}(1 + \beta_m G_m(\zeta)), \quad \tilde{c} = d_3(1 - \varepsilon). \tag{3}$$

Here, β_m is the deformation coefficient and $G_m(\zeta)$ is the Gegenbauer function of first kind. Further, we assume that the coefficient β_m is sufficiently small, so that the higher powers of β_m may be neglected. Under is assumption, the flow of fluid outside the porous region will be governed by the Stokes equation (Happel and Brenner [14]) with continuity condition:

$$\tilde{\nabla}\tilde{p}^o = \tilde{\mu}^o \tilde{\Delta}\tilde{\mathbf{v}}^o, \qquad \tilde{\nabla}.\tilde{\mathbf{v}}^o = 0. \tag{4}$$

The flow of fluid through the porous region will be governed by the Brinkman equation [2], the governing equation for flow inside the porous medium together with continuity condition being

$$\tilde{\nabla}\tilde{p}^i = \tilde{\mu}^i \tilde{\Delta}\tilde{\mathbf{v}}^i - \tilde{k}\tilde{\mathbf{v}}^i, \qquad \tilde{\nabla}.\tilde{\mathbf{v}}^i = 0, \tag{5}$$

where $\tilde{k}$ is the hydrodynamic resistance of the porous region, which is inversely proportional to the hydrodynamic permeability.

3 Solution of the problem

Let us introduce the following non-dimensional variables:

$$\frac{1}{\gamma} = \frac{\tilde{c}}{\tilde{b}}, \quad r = \frac{\tilde{r}}{\tilde{b}}, \quad \nabla = \tilde{\nabla}.\tilde{b}, \quad \Delta = \tilde{\Delta}.\tilde{b}^2, \quad p = \frac{\tilde{p}}{\tilde{p}_o}, \quad \tilde{p}_o = \frac{\tilde{U}.\tilde{\mu}^o}{\tilde{b}}, \quad s = \frac{s_o}{\lambda},$$
$$s_o = \frac{\tilde{b}}{\tilde{R}_b}, \quad \lambda^2 = \frac{\tilde{\mu}^i}{\tilde{\mu}^o}, \quad \nu = \frac{\tilde{\mathbf{v}}}{\tilde{U}}, \quad k = \tilde{k}\tilde{a}^2, \quad \tilde{R}_b = \sqrt{\frac{\tilde{\mu}^o}{\tilde{k}}}, \quad \text{and} \quad \psi^{o,i} = \frac{\tilde{\psi}}{\tilde{U}\tilde{a}^2}. \tag{6}$$

By using the above non-dimensional variables, the governing equations (4)–(5) can be reduced in dimensionless form as:

$$\begin{cases} \nabla p^o = \Delta v^o \\ \nabla . v^o = 0, \end{cases} \tag{7}$$

$$\begin{cases} \nabla p^i = \lambda^2 \Delta v^i - s_0^2 v^i \\ \nabla . v^i = 0. \end{cases} \tag{8}$$

Due to axi-symmetric flow, all the physical quantities are independent of φ. Therefore, the velocity component $\tilde{v}_\varphi$ vanishes along φ-direction. Thus, the non-vanishing velocity components $(v_r, v_\theta, 0)$, satisfying the equations of continuity in both regions, can be defined in terms of stream functions as:

$$v_r^o = \frac{1}{r^2 \sin\theta} \frac{\partial \psi^o}{\partial \theta}; \qquad v_\theta^o = -\frac{1}{r \sin\theta} \frac{\partial \psi^o}{\partial r}, \tag{9}$$

$$v_r^i = \frac{1}{r^2 \sin\theta} \frac{\partial \psi^i}{\partial \theta}; \qquad v_\theta^i = -\frac{1}{r \sin\theta} \frac{\partial \psi^i}{\partial r}. \tag{10}$$

By using Eqs. (9) and (10) in Eqs. (7) and (8), respectively, we can find the stream function formulation of Eqs. (7) and (8) in spherical polar coordinates (r, θ, φ) with the origin located at the centre of the spheroidal particle.

With this formulation, our differential equations (7) and (8) reduce to following fourth-order partial differential equations:

$$E^2(E^2 \psi^o) = 0, \tag{11}$$

$$E^2(E^2 - s^2)\psi^i = 0, \tag{12}$$

where the operator

$$E^2 = \frac{\partial^2}{\partial r^2} + \frac{(1-\zeta^2)}{r^2} \frac{\partial^2}{\partial \zeta^2}, \qquad \zeta = \cos\theta. \tag{13}$$

The tangential and normal stresses (Langlois [33]) for both regions are given by:

$$\sigma_{r\zeta}^o(r,\theta) = \frac{1}{r \sin\theta} \left[\frac{\partial^2 \psi^o}{\partial r^2} - \frac{2}{r} \frac{\partial \psi^o}{\partial r} - \frac{(1-\zeta^2)}{r^2} \frac{\partial^2 \psi^o}{\partial \zeta^2} \right], \tag{14}$$

$$\sigma_{rr}^o = -p^o + 2 \frac{\partial v_r^o}{\partial r}, \tag{15}$$

$$\sigma_{r\zeta}^i(r,\theta) = \frac{\lambda^2}{r \sin\theta} \left[\frac{\partial^2 \psi^i}{\partial r^2} - \frac{2}{r} \frac{\partial \psi^i}{\partial r} - \frac{(1-\zeta^2)}{r^2} \frac{\partial^2 \psi^i}{\partial \zeta^2} \right] \tag{16}$$

$$\sigma_{rr}^i = -p^i + 2\lambda^2 \frac{\partial v_r^i}{\partial r} \tag{17}$$

Now, again using Eqs. (9) and (10) in Eqs. (7) and (8), respectively, we will find the following relations:

$$\frac{\partial p^o}{\partial r} = -\frac{1}{r^2 \sin\theta} \frac{\partial}{\partial \theta}(E^2 \psi^o); \qquad \frac{\partial p^o}{\partial \theta} = \frac{1}{\sin\theta} \frac{\partial}{\partial r}(E^2 \psi^o); \tag{18}$$

$$\frac{\partial p^i}{\partial r} = -\frac{\lambda^2}{r^2 \sin\theta} \frac{\partial}{\partial \theta}(E^2 \psi^i) - s_0^2 v_r^i; \qquad \frac{1}{r} \frac{\partial p^i}{\partial \theta} = \frac{\lambda^2}{r \sin\theta} \frac{\partial}{\partial r}(E^2 \psi^i) - s_0^2 v_\theta^i. \tag{19}$$

Therefore, we can find the pressure in both regions by using Eqs. (18) and (19).

The regular solution of the Stokes equation (11) on the axis of symmetry for axi-symmetric incompressible creeping flow can be expressed (Happel and Brenner [14]) as

$$\psi^o(r,\zeta) = \sum_{n=2}^{\infty} [A_n r^n + B_n r^{-n+1} + C_n r^{-n+3} + D_n r^{n+2}] G_n(\zeta). \tag{20}$$

The complete regular solution of equation (11) on the axis of symmetry for axi-symmetric incompressible slow flow can be expressed (Zlatanovski [26]) as:

$$\psi^i(r,\zeta) = \sum_{n=2}^{\infty} \left[A_n^* r^n + B_n^* r^{-n+1} + C_n^* y_{-n}(sr) + D_n^* y_n(sr)\right] G_n(\zeta), \tag{21}$$

where ψ^i are the stream functions and $G_n(\zeta)$ is the Gegenbauer function of first kind and related to the Legendre function $P_n(\zeta)$ of first kind by the relation

$$G_n(\zeta) = \frac{P_{n-2}(\zeta) - P_n(\zeta)}{(2n-1)}, \quad n \geq 2. \tag{22}$$

Also, we have used the symbols

$$y_{\pm n}(sr) = \sqrt{\frac{\pi r}{2}} s^{\nu} I_{\pm\nu}(sr), \quad \nu = n - \frac{1}{2}, \tag{23}$$

where $I_{\pm\nu}(sr)$ are the modified Bessel functions of first kind and of order ν (Abramowitz and Stegun [34]). In particular, we have

$$\begin{aligned} y_1(sr) &= \sinh(sr), \quad y_2(sr) = s\cosh(sr) - \frac{1}{r}\sinh(sr), \\ y_{-1}(sr) &= \cosh(sr), \; y_{-2}(sr) = \sigma \sinh(sr) - \left(\frac{1}{r}\right)\cosh(sr). \end{aligned} \tag{24}$$

Now, $G_0(\zeta)$ and $G_1(\zeta)$ will not be the part of solution because if we retain the terms multiplied by $G_0(\zeta)$and $G_1(\zeta)$, then velocities will become irregular on the z axis. Therefore, we may now take the stream function inside the porous region as:

$$\begin{aligned} \psi^i = {} & [a_2^* r^2 + b_2^* r^{-1} + c_2^* y_{-2}(sr) + d_2^* y_2(sr)] G_2(\zeta) \\ & + \sum_{n}^{\infty} [A_n^* r^n + B_n^* r^{-n+1} + C_n^* y_{-n}(sr) + D_n^* y_n(sr)] G_n(\zeta), \end{aligned} \tag{25}$$

while the stream function outside the porous region can be taken as:

$$\psi^o = [a_2 r^2 + \frac{b_2}{r} + c_2 r + d_2 r^4] G_2(\zeta) + \sum_{n}^{\infty} [A_n r^n + B_n r^{-n+1} + C_n r^{-n+3} + D_n r^{n+2}] G_n(\zeta). \tag{26}$$

It is important to note that the coefficients $a_2, b_2, c_2, d_2, a_2^*, b_2^*, c_2^*$ and d_2^* contribute to the flow past an impermeable sphere composed by a porous layer (Yadav, et al. [12]), and consequently, we expect that all other coefficients in (25) and (26) are of order β_m. Therefore, except where these coefficients enter, we may take the surface to be perfect sphere instead of either of their exact forms (1) or (2).

Boundary conditions

In order to find the solution of the above boundary value problem, it is necessary to define suitable boundary conditions which are physically realistic and mathematically consistent. The suitable boundary conditions for this problem are continuity of velocity components and normal stress along with the discontinuity in tangential stress at $r = 1 + \beta_m G_m(\zeta)$, which was proved by Ochoa-Tapia and Whitaker [35,36] with the help of the volume averaging technique and continuity of the radial components of the fluid velocity on the outer cell surface with suitable assumption of cell model technique for different models.

Mathematically,

On the impermeable surface $r = \ell(1 + \beta_m G_m(\zeta))$

$$v_r^i = 0, \quad v_\theta^i = 0. \tag{27}$$

On the porous surface $r = 1 + \beta_m G_m(\zeta)$

continuity of velocity components:

$$v_r^o = v_r^i, \quad v_\theta^o = v_\theta^i, \tag{28}$$

continuity of normal stress:

$$-p^o + 2\frac{\partial v_r^o}{\partial r} = -p^i + 2\lambda^2 \frac{\partial v_r^i}{\partial r}, \tag{29}$$

stress jump condition:

$$\lambda^2 \left(\frac{1}{r}\frac{\partial v_r^i}{\partial \theta} + \frac{\partial v_\theta^i}{\partial r} - \frac{v_\theta^i}{r} \right) - \left(\frac{1}{r}\frac{\partial v_r^o}{\partial \theta} + \frac{\partial v_\theta^o}{\partial r} - \frac{v_\theta^o}{r} \right) = \frac{\beta}{\sqrt{k}} v_\theta^i. \tag{30}$$

On the hypothetical cell surface: $r = \frac{1}{\gamma}(1 + \beta_m G_m(\zeta))$

The continuity of the radial components of fluid velocity:

$$v_r^o = \cos\theta. \tag{31}$$

Assumption of cell model technique for different models:
Happel [6,7] assumes that the tangential stress vanishes on the outer cell surface:

$$\sigma_{r\zeta}^o(r,\theta) = 0, \quad \text{i.e.,} \quad \frac{\partial^2 \psi^o}{\partial r^2} - \frac{2}{r}\frac{\partial \psi^o}{\partial r} - \frac{(1-\zeta^2)}{r^2}\frac{\partial^2 \psi^o}{\partial \zeta^2} = 0, \tag{32}$$

Kuwabara [8] assumes that the vorticity is zero on the outer cell surface, i.e. the curl of the velocity vector ($\tilde{\mathbf{v}}^o$) vanishes on the outer cell surface:

$$\text{rot}(\tilde{\mathbf{v}}^o) = 0 \text{ i.e.} \frac{\partial^2 \psi^o}{\partial r^2} + \frac{(1-\zeta^2)}{r^2}\frac{\partial^2 \psi^o}{\partial \zeta^2} = 0, \tag{33}$$

Kvashnin [11] introduced a symmetry condition on the outer cell surface:

$$\frac{\partial v_\theta^o}{\partial r} = 0, \tag{34}$$

Mehta–Morse [9] assumes homogeneity of the flow on the outer cell surface:

$$v_\theta^o = -\sin\theta. \tag{35}$$

Determination of arbitrary constants
With the help of stream function given by Eqs. (25) and (26) for both the regions respectively, we can obtain the components of velocity, shear and normal stress and pressure for both regions by using formulae (9)–(10) and (14)–(19). Substituting the values of p^o,p^i,v_r^0, v_r^i, v_θ^o, v_θ^i, $\sigma_{r\zeta}^o(r,\theta)$ and $\sigma_{r\zeta}^i(r,\theta)$ in Eqs. (27)–(35) and using the following identities:

$$y_n'(sr) = s^2 y_{n-1}(sr) + \frac{1-n}{r} y_n(sr), \quad y_{-n}'(sr) = s^2 y_{-n+1}(sr) + \frac{1-n}{r} y_{-n}(sr),$$

$$y_n''(sr) = \left[s^2 + \frac{n(n-1)}{r^2} \right] y_n(sr), \quad y_{-n}''(sr) = \left[s^2 + \frac{n(n-1)}{r^2} \right] y_{-n}(sr),$$

$$G_m(\zeta)G_2(\zeta) = -\frac{(m-2)(m-3)}{2(2m-1)(2m-3)} G_{m-2}(\zeta) + \frac{m(m-1)}{(2m+1)(2m-3)} G_m(\zeta) - \frac{(m+1)(m+2)}{2(2m-1)(2m+1)} G_{m+2}(\zeta),$$

$$P_1(\zeta)G_m(\zeta) = \frac{(m-2)}{(2m-1)(2m-3)} P_{m-3}(\zeta) + \frac{1}{(2m+1)(2m-3)} P_{m-1}(\zeta) - \frac{(m+1)}{(2m+1)(2m-1)} P_{m+1}(\zeta),$$

we obtain

$$[\ell^3 a_2^* + b_2^* + \ell y_{-2}(s\ell)c_2^* + \ell y_2(s\ell)d_2^*]P_1(\zeta) + [3\ell^3 a_2^* + s^2\ell^2 y_{-1}(s\ell)c_2^* + s^2\ell^2 y_1(s\ell)d_2^*]$$
$$\beta_m(\zeta)G_m(\zeta)P_1(\zeta) + \sum_n^\infty [\ell^{n+1}A_n^* + \ell^{-n+2}B_n^* + \ell y_{-n}(s\ell)C_n^* + \ell y_{-n}(s\ell)D_n^*]P_{n-1}(\zeta) = 0, \tag{36}$$

$$[2\ell^3 a_2^* - b_2^* + (s^2\ell^2 y_{-1}(s\ell) - \ell y_{-2}(s\ell))c_2^* + (s^2\ell^2 y_1(s\ell) - \ell y_2(s\ell))d_2^*]G_2(\zeta)$$
$$+ [6\ell^3 a_2^* + \{s^2\ell^3 y_{-2}(s\ell) + 2s^2\ell^2 y_{-1}(s\ell)\}c_2^* + \{s^2\ell^3 y_2(s\ell) + 2s^2\ell^2 y_1(s\ell)\}d_2^*]\beta_m(\zeta)$$
$$G_m(\zeta)G_2(\zeta) + \sum_n^\infty [n\ell^{n+1}A_n^* + (1-n)\ell^{-n+2}B_n^* + \ell^2 y'_{-n}(s\ell)C_n^* + \ell^2 y'_n(s\ell)D_n^*]G_n(\zeta) = 0, \tag{37}$$

$$[a_2 + b_2 + c_2 + d_2 - a_2^* - b_2^* - d_2^* y_{-2}(s) - d_2^* y_2(s)]P_1(\zeta) + [2a_2 - b_2 + c_2 + 4d_2 - 2a_2^* + b_2^*$$
$$+ c_2^*(y_{-2}(s) - s^2 y_{-1}(s)) + d_2^*(y_2(s) - s^2 y_1(s))]\beta_m(\zeta)G_m(\zeta)P_1(\zeta)$$
$$+ \sum_n^\infty [A_n + B_n + C_n + D_n - A_n^* - B_n^* - C_n^* y_{-n}(s) - D_n^* y_n(s)]P_{n-1}(\zeta) = 0, \tag{38}$$

$$[2a_2 - b_2 + c_2 + 4d_2 - 2a_2^* + b_2^* - c_2^*(s^2 y_{-1}(s) - y_{-2}(s)) - d_2^*(s^2 y_1(s) - y_2(s))]G_2(\zeta)$$
$$+ [2a_2 + 2b_2 + 12d_2 - 2a_2^* - 2b_2^* - c_2^*(s^2+2)y_{-2}(s) - d_2^*(s^2+2)y_2(s)]\beta_m(\zeta)G_2(\zeta)G_m(\zeta)$$
$$+ \sum_n^\infty [nA_n + (1-n)B_n + (3-n)C_n + (n+2)D_n - nA_n^* - (1-n)B_n^* - C_n^*\{s^2 y_{-n+1}(s) + (1-n)y_{-n}(s)\}$$
$$- D_n^*(s^2 y_{n-1}(s) + (1-n)y_n(s))]G_n(\zeta) = 0, \tag{39}$$

$$[12b_2 + 6c_2 + 12d_2 + 2s^2\lambda^2 a_2^* - (s^2\lambda^2 + 12\lambda^2)b_2^* - \{12\lambda^2 y_{-2}(s) - 4\lambda^2 s^2 y_{-1}(s)\}c_2^*$$
$$- \{12\lambda^2 y_2(s) - 4\lambda^2 s^2 y_1(s)\}d_2^*]P_1(\zeta) + [-12b_2 + 6c_2 + 48d_2 + 8\lambda^2 s^2 a_2^* - (s^2\lambda^2 - 12\lambda^2)b_2^*$$
$$+ \{(4s^2\lambda^2 + 12\lambda^2)y_{-2}(s) - 4s^2\lambda^2 y_{-1}(s)\}c_2^* + \{(4s^2\lambda^2 + 12\lambda^2)y_2(s) - 4s^2\lambda^2 y_1(s)\}d_2^*]\beta_m(\zeta)G_m(\zeta)P_1(\zeta)$$
$$+ \sum_n^\infty 4(2-n)A_n + 4(n+1)B_n + \frac{4(n^2+n-3)}{n}C_n + \frac{4(n^2-3n-1)}{1-n}D_n$$
$$+ \left\{\frac{2\lambda^2 s^2}{n-1} + 4\lambda^2(n-2)\right\}A_n^* - \left\{\frac{2\lambda^2 s^2}{n} + 4\lambda^2(n+1)\right\}B_n^* + \{4\lambda^2 s^2 y_{-n+1}(s) - 4\lambda^2(n+1)y_{-n}(s)\}C_n^*$$
$$+ \{4\lambda^2 s^2 y_{n-1}(s) - \lambda^2(n+1)y_n(s)\}D_n^*]G_m(\zeta) = 0, \tag{40}$$

$$\Bigg[- 6b_2 - 6d_2 - \frac{2\beta}{\sqrt{k}}a_2^* + (6\lambda^2 + \frac{\beta}{\sqrt{k}})b_2^* + \left\{(\lambda^2((s^2+6)y_{-2}(s) - 2s^2 y_{-1}(s)) - \frac{\beta}{\sqrt{k}}(s^2 y_{-1}(s) - y_{-2}(s))\right\}c_2^*$$
$$+ \left\{(\lambda^2((s^2+6)y_2(s) - 2s^2 y_1(s)) - \frac{\beta}{\sqrt{k}}(s^2 y_1(s) - y_2(s))\right\}d_2^*\Bigg]G_2(\zeta) + [6b_2 - 24d_2 - \frac{6\beta}{\sqrt{k}}a_2^* - 6\lambda^2 b_2^*$$
$$+ \left\{\lambda^2((s^4+2s^2)y_{-1}(s) - (s^2+6)y_{-2}(s)) - \frac{\beta}{\sqrt{k}}s^2(2y_{-1}(s) + y_{-2}(s))\right\}c_2^* + \{\lambda^2((s^4+2s^2)y_1(s) - (s^2+6)y_2(s))$$
$$- \frac{\beta}{\sqrt{k}}s^2(2y_1(s) + y_2(s))\}d_2^*]\beta_m(\zeta)G_m(\zeta)G_2(\zeta) + \sum_n^\infty [-2n(n-2)A_n - 2(n^2-1)B_n - 2n(n-2)C_n - 2(n^2-1)D_n$$
$$+ (\lambda^2(2n^2 - 4n) - \frac{\beta}{\sqrt{k}}n)A_n^* + \{2\lambda^2(n^2-1) + \frac{\beta}{\sqrt{k}}(n-1)\}B_n^* + \{\lambda^2((s^2 + 2n^2 - 2)y_{-n}(s) - 2s^2 y_{-n+1}(s))$$
$$- \frac{\beta}{\sqrt{k}}(s^2 y_{-n+1}(s) + (1-n)y_{-n}(s))\}C_n^* + \{\lambda^2((s^2 + 2n^2 - 2)y_n(s) - 2s^2 y_{n-1}(s))$$
$$- \frac{\beta}{\sqrt{k}}(s^2 y_{n-1}(s) + (1-n)y_n(s))\}D_n^*]G_m(\zeta) = 0, \tag{41}$$

$$[a_2\gamma^2 + b_2\gamma^5 + c_2\gamma^3 + d_2 + \gamma^2]P_1(\zeta) - \Bigg[3b_2\gamma^5 + c_2\gamma^3 - 2d_2]\beta_m(\zeta)G_m(\zeta)P_1(\zeta) + \sum_n^\infty [A_n\gamma^{4-n}$$
$$+ B_n\gamma^{n+3} + C_n\gamma^{n+1} + D_n\gamma^{2-n}\Bigg]P_{n-1}(\zeta) = 0. \tag{42}$$

Happel's boundary condition:

$$[6b_2\gamma^5 + 6d_2]G_2(\zeta) + [24b_2\gamma^5 + 6d_2]\beta_m(\zeta)G_m(\zeta)G_2(\zeta) + \sum_n^\infty[(2n^2-4n)A_n\gamma^{4-n} + (2n^2-2)B_n\gamma^{n+3} + (2n^2-4n)C_n\gamma^{n+1} + (2n^2-2)D_n\gamma^{2-n}]G_m(\zeta) = 0. \tag{43}$$

Kuwabara's boundary condition:

$$[-2\gamma^3c_2 + 10d_2]G_2(\zeta) + [2\gamma^3c_2 + 20d_2]\beta_m(\zeta)G_m(\zeta)G_2(\zeta) + \sum_n^\infty[(6-4n)\gamma^{n+1}C_n + (4n+2)\gamma^{2-n}D_n]G_m(\zeta) = 0. \tag{44}$$

Kvashnin's boundary condition:

$$[3\gamma^5b_2 - \gamma^3c_2 + 8d_2]G_2(\zeta) + [-12\gamma^5b_2 + 2\gamma^3c_2 + 8d_2]\beta_m(\zeta)G_m(\zeta)G_2(\zeta) + \sum_n^\infty[n(n-2)\gamma^{4-n}A_n + (n^2-1)\gamma^{n+3}B_n + (n-1)(n-3)\gamma^{n+1}C_n + n(n+2)\gamma^{2-n}D_n]G_m(\zeta) = 0. \tag{45}$$

Mehta–Morse's boundary condition:

$$[2\gamma^2a_2 - \gamma^5b_2 + \gamma^3c_2 + 4d_2 + 2\gamma^2]G_2(\zeta) + [3\gamma^5b_2 - \gamma^3c_2 + 8d_2]\beta_m(\zeta)G_m(\zeta)G_2(\zeta) + \sum_n^\infty[n\gamma^{4-n}A_n + (1-n)\gamma^{n+3}B_n + (3-n)\gamma^{n+1}C_n + (n+2)\gamma^{2-n}D_n]G_m(\zeta) = 0. \tag{46}$$

In this way, we obtain seven equations containing eight arbitrary constants in leading terms. Thus, the values of the arbitrary constants appearing in the leading terms will depend on the selection of the model used, i.e. on the boundary conditions (43)–(46). All the arbitrary constants can be obtained by using the perturbation method.

Solving the leading terms in Eqs. (36)–(42) by taking each model, respectively, with the help of Mathematica software, we can find the arbitrary constants a_2, b_2, c_2, d_2, a_2^*, b_2^*, c_2^* and d_2^*. Substituting these values corresponding to each model into Eqs. (36)–(46), we have

$$\sum_n^\infty[\ell^{n+1}A_n^* + \ell^{-n+2}B_n^* + \ell y_{-n}(s\ell)C_n^* + \ell y_{-n}(s\ell)D_n^*]P_{n-1}(\zeta) = 0, \tag{47}$$

$$\sum_n^\infty[n\ell^{n+1}A_n^* + (1-n)\ell^{-n+2}B_n^* + \ell^2y'_{-n}(s\ell)C_n^* + \ell^2y'_n(s\ell)D_n^*]G_n(\zeta) = p_2\beta_m[E_{m-2}G_{m-2}(\zeta) + E_mG_m(\zeta) + E_{m+2}G_{m+2}(\zeta)], \tag{48}$$

$$\sum_n^\infty[A_n + B_n + C_n + D_n - A_n^* - B_n^* - C_n^*y_{-n}(s) - D_n^*y_n(s)]P_{n-1}(\zeta) = 0, \tag{49}$$

$$\sum_n^\infty[nA_n + (1-n)B_n + (3-n)C_n + (n+2)D_n - nA_n^* - (1-n)B_n^* - C_n^*\{s^2y_{-n+1}(s) + (1-n)y_{-n}(s)\} - D_n^*(s^2y_{n-1}(s) + (1-n)y_n(s))]G_n(\zeta) = q_2\beta_m[E_{m-2}G_{m-2}(\zeta) + E_mG_m(\zeta) + E_{m+2}G_{m+2}(\zeta)], \tag{50}$$

$$\sum_n^\infty 4(2-n)A_n + 4(n+1)B_n + \frac{4(n^2+n-3)}{n}C_n + \frac{4(n^2-3n-1)}{1-n}D_n + \left\{\frac{2\lambda^2s^2}{n-1} + 4\lambda^2(n-2)\right\}A_n^* - \left\{\frac{2\lambda^2s^2}{n} + 4\lambda^2(n+1)\right\}B_n^* + \{4\lambda^2s^2y_{-n+1}(s) - 4\lambda^2(n+1)y_{-n}(s)\}C_n^* + \{4\lambda^2s^2y_{n-1}(s) - \lambda^2(n+1)y_n(s)\}D_n^*]G_m(\zeta) = s_2\beta_m[T_{m-2}P_{m-3}(\zeta) + T_mP_{m-1}(\zeta) + T_{m+2}P_{m+1}(\zeta)], \tag{51}$$

$$\sum_{n}^{\infty}[-2n(n-2)A_n - 2(n^2-1)B_n - 2n(n-2)C_n - 2(n^2-1)D_n + \left(\lambda^2(2n^2-4n) - \frac{\beta}{\sqrt{k}}n\right)A_n^*$$
$$+\{2\lambda^2(n^2-1) + \frac{\beta}{\sqrt{k}}(n-1)\}B_n^* + \{\lambda^2((s^2+2n^2-2)y_{-n}(s) - 2s^2y_{-n+1}(s)) - \frac{\beta}{\sqrt{k}}(s^2y_{-n+1}(s)$$
$$+(1-n)y_{-n}(s))\}C_n^* + \{\lambda^2((s^2+2n^2-2)y_n(s) - 2s^2y_{n-1}(s))$$
$$-\frac{\beta}{\sqrt{k}}(s^2y_{n-1}(s) + (1-n)y_n(s))\}D_n^*]G_m(\zeta)$$
$$= u_2\beta_m[E_{m-2}G_{m-2}(\zeta) + E_mG_m(\zeta) + E_{m+2}G_{m+2}(\zeta)], \tag{52}$$

$$\sum_{n}^{\infty}[A_n\gamma^{4-n} + B_n\gamma^{n+3} + C_n\gamma^{n+1} + D_n\gamma^{2-n}]P_{n-1}(\zeta)$$
$$= w_2\beta_m[T_{m-2}P_{m-3}(\zeta) + T_mP_{m-1}(\zeta) + T_{m+2}P_{m+1}(\zeta)]. \tag{53}$$

Happel's boundary condition:

$$\sum_{n}^{\infty}[(2n^2-4n)A_n\gamma^{4-n} + (2n^2-2)B_n\gamma^{n+3} + (2n^2-4n)C_n\gamma^{n+1} + (2n^2-2)D_n\gamma^{2-n}]G_m(\zeta)$$
$$= t_2\beta_m[E_{m-2}G_{m-2}(\zeta) + E_mG_m(\zeta) + E_{m+2}G_{m+2}(\zeta)]. \tag{54}$$

Kuwabara's boundary condition:

$$\sum_{n}^{\infty}[(6-4n)\gamma^{n+1}C_n + (4n+2)\gamma^{2-n}D_n]G_m(\zeta)$$
$$= t_2\beta_m[E_{m-2}G_{m-2}(\zeta) + E_mG_m(\zeta) + E_{m+2}G_{m+2}(\zeta)]. \tag{55}$$

Kvashnin's boundary condition:

$$\sum_{n}^{\infty}[n(n-2)\gamma^{4-n}A_n + (n^2-1)\gamma^{n+3}B_n + (n-1)(n-3)\gamma^{n+1}C_n + n(n+2)\gamma^{2-n}D_n]G_m(\zeta)$$
$$= t_2\beta_m[E_{m-2}G_{m-2}(\zeta) + E_mG_m(\zeta) + E_{m+2}G_{m+2}(\zeta)]. \tag{56}$$

Mehta–Morse's boundary condition:

$$\sum_{n}^{\infty}[n\gamma^{4-n}A_n + (1-n)\gamma^{n+3}B_n + (3-n)\gamma^{n+1}C_n + (n+2)\gamma^{2-n}D_n]G_m(\zeta)$$
$$= t_2\beta_m[E_{m-2}G_{m-2}(\zeta) + E_mG_m(\zeta) + E_{m+2}G_{m+2}(\zeta)], \tag{57}$$

where

$$p = 2c_2 - 10d_2 + s^2b_1d_2^*,$$
$$q_2 = 2c_2 - 10d_2 + s^2y_{-2}(s)c_2^* + s^2y_2(s)\,d_2^*,$$
$$s_2 = [24b_2 - 36d_2 - 6\lambda^2s^2a_2^* - 24\lambda^2b_2^* - \{(4s^2\lambda^2 + 12\lambda^2)y_{-2}(s) - 8s^2\lambda^2y_{-1}(s)\}c_2^*$$
$$-\{(4s^2\lambda^2 + 12\lambda^2)y_2(s) - 8s^2\lambda^2y_1(s)\}d_2^*],$$
$$u_2 = [30d_2 + \frac{8\beta}{\sqrt{k}}a_2^* + \frac{\beta}{\sqrt{k}}b_2^* - \{\lambda^2s^4y_{-1}(s) - \frac{3\beta}{\sqrt{k}}s^2y_{-1}(s) + \frac{\beta}{\sqrt{k}}(1-s^2)y_{-2}(s)\}c_2^*$$
$$-\{\lambda^2s^4y_1(s) - \frac{3\beta}{\sqrt{k}}s^2y_1(s) + \frac{\beta}{\sqrt{k}}(1-s^2)y_2(s)\}d_2^*,$$

$$w_2 = \begin{cases} c_2\gamma^3 - 5d_2, & \text{for the Happel model} \\ 3b_2\gamma^5 + 3d_2, & \text{for the Kuwabara model} \\ 2c_2\gamma^3 - 10d_2, & \text{for the Kvashnin model} \\ 0, & \text{for the Mehta–Morse model} \end{cases}$$

$$t_2 = \begin{cases} -30d_2, & \text{for the Happel model} \\ -30d_2, & \text{for the Kuwabara model} \\ 2c_2\gamma^3 - 40d_2, & \text{for the Kvashnin model} \\ 2c_2\gamma^3 - 10d_2, & \text{for the Mehta–Morse model} \end{cases}$$

$$E_{m-2} = -\frac{m-3}{2}T_{m-2},\ E_m = m(m-1)T_m,\quad E_{m+2} = \frac{m+2}{2}T_{m+2},$$
$$T_{m-2} = \frac{m-2}{(2m-1)(2m-3)},\ T_m = \frac{1}{(2m+1)(2m-3)},\ T_{m+2} = \frac{1+m}{(2m+1)(1-2m)}.$$

The non-vanishing coefficients A_n, B_n, C_n, D_n, A_n^*, B_n^*, C_n^* and D_n^* which correspond to $n = m-2, m, m+2$ can be obtained from Eqs. (47)–(53) together with one of the models (54)–(57).

Therefore, we have determined the explicit expression for the stream functions for the flow outside and inside of the porous deformed spheroid as:

$$\begin{aligned}\psi^o =& \left[a_2r^2 + \frac{b_2}{r} + c_2r + d_2r^4\right]G_2(\zeta) + [A_{m-2}r^{m-2} + B_nr^{-m+3} + C_{m-2}r^{-m+5} + D_{m-2}r^{-m+4}]G_{m-2}(\zeta) \\ &+ \left[A_mr^m + B_mr^{-m+1} + C_mr^{-m+3} + D_mr^{m+2}\right]G_m(\zeta) + [A_{m+2}r^{m+2} + B_{m+2}r^{-m-1} + C_{m+2}r^{-m+1} \\ &+ D_{m+2}r^{m+4}]G_{m+2}(\zeta), \end{aligned} \tag{58}$$

$$\begin{aligned}\psi^i =& \left[a_2^*r^2 + b_2^*r^{-1} + c_2^*y_{-2}(sr) + d_2^*y_2(sr)\right]G_2(\zeta) + [A_{m-2}^*r^{m-2} + B_{m-2}^*r^{-m+3} \\ &+ C_{m-2}^*y_{-m+2}(sr) + D_{m-2}^*y_{m-2}(sr)]G_{m-2}(\zeta) + [A_m^*r^m + B_m^*r^{-m+1} + C_m^*y_{-m}(sr) \\ &+ D_m^*y_m(sr)]G_m(\zeta) + \left[A_{m+2}^*r^{m+2} + B_{m+2}^*r^{-m-1} + C_{m+2}^*y_{-m-2}(sr)D_{m+2}^*y_{m+2}(sr)\right]G_{m+2}(\zeta). \end{aligned} \tag{59}$$

3.1 Hydrodynamic permeability of a membrane built up by an impermeable oblate spheroid coated by a porous layer

Here, we consider the steady, axi-symmetric flow of viscous, incompressible fluid through an impermeable oblate spheroid coated with a porous layer as a particular example of the preceding analysis. The Cartesian equation of a porous oblate spheroid enclosing an impermeable spheroid can be taken as

$$\frac{x^2+y^2}{d^2} + \frac{z^2}{d^2(1-\varepsilon)^2} = 1, \tag{60}$$

where d is the equatorial radius of the porous oblate spheroid and ε is the deformation parameter which we will take very small so that we can omit the squares and higher powers of ε. The polar form of the equation of the porous oblate spheroid can be written as

$$\tilde{r} = \tilde{b}(1 + 2\varepsilon G_2(\zeta)). \tag{61}$$

Here, it may be mentioned that for $\varepsilon > 0$, the shape of the spheroid will be oblate, whereas for $\varepsilon < 0$ the shape will become prolate. Comparison with Eq. (1) leads to the values of $m = 2$, $\beta_m = 2\varepsilon$.

Since $A_0, B_0, C_0, D_0, A_0^*, B_0^*, C_0^*, D_0^*$ all become zero and further using (61), we find from Eqs. (58) and (59) that the stream functions around and through the porous oblate spheroid enclosing an impermeable spheroid are

$$\begin{aligned}\psi^o =& \left[a_2r^2 + \frac{b_2}{r} + c_2r + d_2r^4\right]G_2(\zeta) \\ &+ \left[A_2r^2 + B_2r^{-1} + C_2r + D_2r^4\right]G_2(\zeta) + \left[A_4r^4 + B_4r^{-3} + C_4r^{-1} + D_4r^6\right]G_4(\zeta), \end{aligned} \tag{62}$$

$$\begin{aligned}\psi^i =& \left[a_2^*r^2 + b_2^*r^{-1} + c_2^*y_{-2}(sr) + d_2^*y_2(sr)\right]G_2(\zeta) + \left[A_2^*r^2 + B_2^*r^{-1} + C_2^*y_{-2}(sr) + D_2^*y_2(sr)\right]G_2(\zeta) \\ &+ \left[A_4^*r^4 + B_4^*r^{-3} + C_4^*y_{-4}(sr) + D_4^*y_4(sr)\right]G_4(\zeta). \end{aligned} \tag{63}$$

Investigation of flow in concentrated dispersive systems, built up by porous oblate spheroidal particles enclosing a solid core (into which any membranes also fall), is important for both natural and industrial processes. In this paper, we are interested to see the effect of particle volume fraction, deformation parameter, viscosity and permeability of the porous medium, etc., on the drag force exerted by the fluid on the membrane and the hydrodynamic permeability of the membrane.

The drag force experienced by the porous oblate spheroid enclosing a solid core under the condition of stress jump can be investigated by using the formula (Happel and Brenner, [14], p. 115) as

$$\tilde{F} = \pi \tilde{\mu}^o \tilde{U} \tilde{b} \int_0^{\pi} \varpi^3 \frac{\partial}{\partial r} \left(\frac{E^2 \psi^o}{\varpi^2} \right) r \mathrm{d}\theta. \tag{64}$$

Here, $\varpi = r \sin\theta$ and

$$E^2 \psi^o = -2 \left[\left\{ (c_2 + C_2) \left(\frac{1}{r} \right) - 5(d_2 + D_2) r^2 \right\} G_2(\zeta) + \left\{ 5C_4 \frac{1}{r^3} - 9D_4 r^4 \right\} G_4(\zeta) \right]. \tag{65}$$

Using the value of $E^2 \psi^o$ in Eq. (64) and integrating, we get the drag force experienced by the porous oblate spheroid enclosing a solid core as:

$$\tilde{F} = 4\pi \tilde{\mu}^o d \tilde{U} [(1 - \varepsilon) c_2 + C_2]. \tag{66}$$

It is important to note that only the Stokes coefficients c_2 and C_2 of the stream function contribute to the drag force. The values of c_2 for each model can be obtained by solving the leading terms of Eqs. (36)–(42) with one of the Eqs. (43)–(46). Solving Eqs. (47)–(53) with one of the Eqs. (54)–(57) for $m = 2$, we can find the values of A_2, B_2, C_2, D_2, A_2^*, B_2^*, C_2^*, D_2^*, A_4, B_4, C_4, D_4, A_4^*, B_4^*, C_4^* and D_4^*.

The hydrodynamic permeability of a membrane $\tilde{L}_{11}$ is defined as the ratio of the uniform flow rate $\tilde{U}$ to the cell gradient pressure $\tilde{F}/\tilde{V}$ [14]:

$$\tilde{L}_{11} = \frac{\tilde{U}}{\tilde{F}/\tilde{V}}, \tag{67}$$

with $\tilde{V} = \frac{4}{3}\pi d_2^2 \tilde{c}$ being the volume of the cell.

Substituting the value of $\tilde{F}$ from Eq. (66) and the value of $\tilde{V}$ from above into (67), we obtain the hydrodynamic permeability of a membrane as:

$$\tilde{L}_{11} = \frac{1}{3\gamma^3} \frac{(1 - \varepsilon)}{\{(1 - \varepsilon) c_2 + C_2\}} \frac{d^2}{\tilde{\mu}^o} = L_{11} \frac{d^2}{\tilde{\mu}^o}, \tag{68}$$

with $L_{11} = \frac{1}{3\gamma^3} \frac{(1-\varepsilon)}{\{(1-\varepsilon)c_2 + C_2\}}$ being the dimensionless hydrodynamic permeability of a membrane. By substituting the value of C_1 and C_2 for all models in the above equation, respectively, we can obtain the dimensionless hydrodynamic permeability of a membrane for all models.

The effect of penetrability s on the non-dimensional hydrodynamic permeability, L_{11}, of a membrane constructed by impermeable oblate spheroidal particles covered by a porous layer is shown in Fig. 2. This figure shows that the non-dimensional hydrodynamic permeability, L_{11}, of a membrane decreases with increasing penetrability parameter s for all four models, at $\gamma = 0.8$, $\lambda = 1$, $\varepsilon = 0.05$, $\ell = 0.5$, $k = 0.5$ and $\beta = 0.5$. From the graph, it is also observed that the rate of decrease in the hydrodynamic permeability of a membrane for Mehta–Morse's model is higher than for the other three models.

The variation of the natural logarithm of the non-dimensional hydrodynamic permeability, L_{11}, of a membrane with the viscosity ratio λ in the cell for all four models, at $\gamma = 0.4$, $s = 5$, $\varepsilon = 0.1$, $\ell = 0.5$, $k = 0.5$ and $\beta = 0.5$, is explained in Fig. 3. From the graph, we can reach the interpretation that the hydrodynamic permeability of a membrane decreases by increasing the viscosity ratio, i.e., the flow of the fluid becomes difficult with increasing inner viscosity. Also, we found that the nature of graph's turn means that the decrease in hydrodynamic permeability slows down with viscosity ratio if we take $\gamma = 0.5$ or more.

Figure 4 represents the inter-dependence of the natural logarithm of the non-dimensional hydrodynamic permeability, L_{11}, of a membrane with cell volume fraction γ for all four models, at $\lambda = 2$, $s = 4$, $\varepsilon = 0.1$ and $\beta = 0.5$. The graph shows that the hydrodynamic permeability of a membrane in the cell decreases by increasing the particle volume fraction γ. Also we are getting the interpretation that the rate of decrease in L_{11}

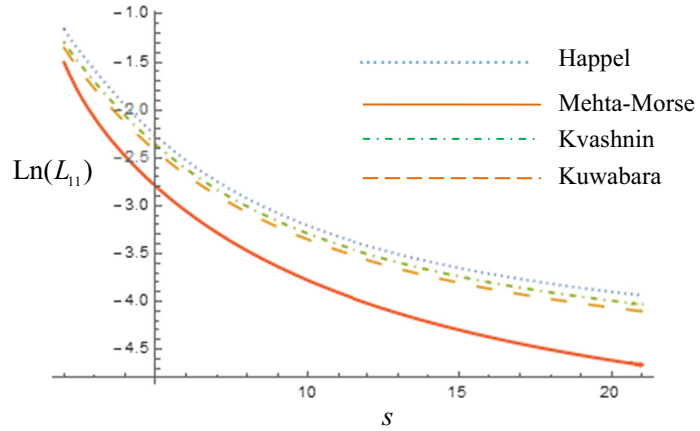

Fig. 2 Variation of natural logarithm of the dimensionless hydrodynamic permeability, L_{11}, of a membrane with parameter s for the all four models at, $\gamma = 0.8$, $\lambda = 1$, $\varepsilon = 0.05$, $\ell = 0.5$, $k = 0.5$ and $\beta = 0.5$

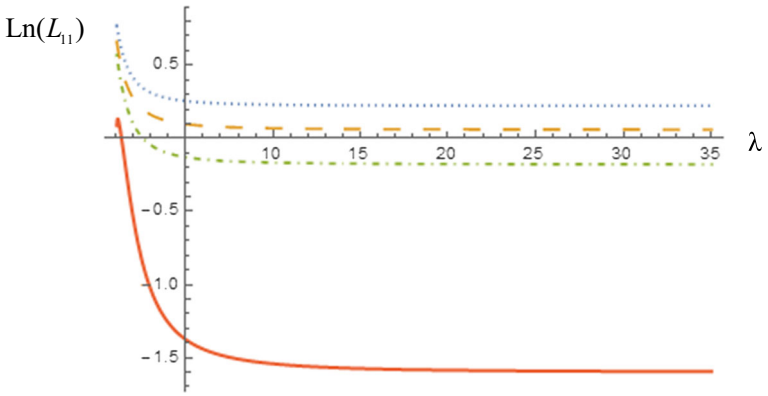

Fig. 3 Variation of natural logarithm of the dimensionless hydrodynamic permeability, L_{11}, of a membrane with parameter λ for all four models at, $\gamma = 0.4$, $s = 5$, $\varepsilon = 0.1$, $\ell = 0.5$, $k = 0.5$ and $\beta = 0.5$

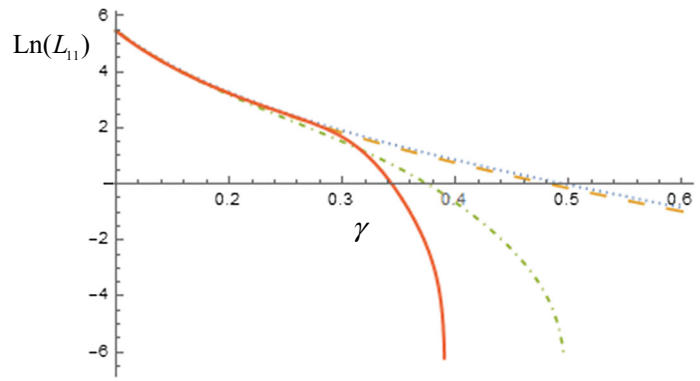

Fig. 4 Dependence of natural logarithm of the dimensionless hydrodynamic permeability, L_{11}, of a membrane with parameter γ for all models at, $\lambda = 2$, $s = 4$, $\varepsilon = 0.1$, $\ell = 0.5$, $k = 0.5$ and $\beta = 0.5$

is low for high values of particle volume fraction γ for Kuwabara's and Kvashnin's model and almost equal; it is high for high values of particle volume fraction γ for Happel's and Mehta–Morse's model; and all four models agree on a very low particle volume fraction, which is similar to the case of a membrane built up by spherical and cylindrical particles. The effect of the deformation coefficient ε on the natural logarithm of the non-dimensional hydrodynamic permeability, L_{11}, of a membrane for all four models, at $\lambda = 1, s = 5, \gamma = 0.6$ and $\beta = 0.5$, is discussed in Fig. 5. This figure shows that the hydrodynamic permeability of a membrane

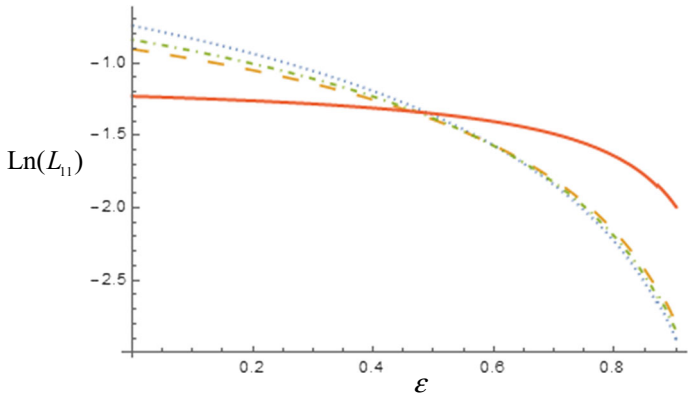

Fig. 5 Variation of natural logarithm of the dimensionless hydrodynamic permeability, L_{11}, of a membrane with parameter ε for all models at, $\lambda = 1$, $s = 5$, $\gamma = 0.6$, $\ell = 0.5$, $k = 0.5$ and $\beta = 0.5$

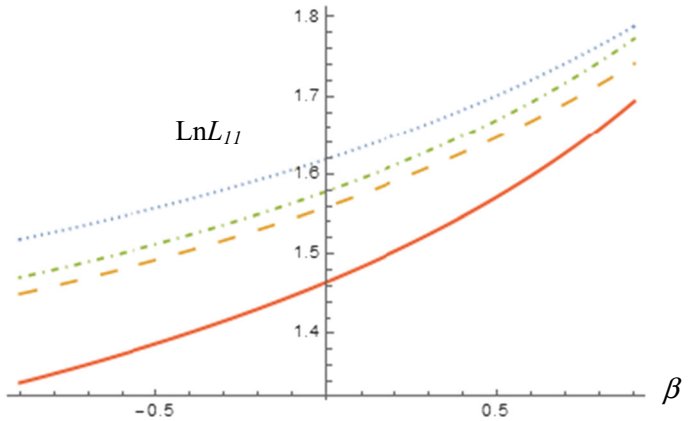

Fig. 6 Variation of natural logarithm of the dimensionless hydrodynamic permeability, L_{11}, of a membrane with the stress jump coefficient β at $\gamma = 0.3$, $\varepsilon = 0.3$ $s = 5$, $\ell = 0.5$, $k = 0.5$ and $\lambda = 1$

decreases with an increase of the deformation parameter ε. The value of the hydrodynamic permeability of a membrane for Mehta–Morse's model is higher than the value of hydrodynamic permeability of a membrane for the other three models for higher deformation parameter.

The effect of the stress jump coefficient on the non-dimensional hydrodynamic permeability, L_{11}, of a membrane for all four models is shown in Fig. 6 when $\lambda = 1$, $\gamma = 0.3$, $s = 5$, $\varepsilon = 0.3$, $\ell = 0.5$ and $k = 0.5$. From the graph, we can reach the interpretation that the hydrodynamic permeability of a membrane increases by increasing the stress jump coefficient.

3.2 Hydrodynamic permeability of a membrane built up by porous oblate spheroid

In this section, we consider a membrane (Fig. 7a) built up by porous oblate spheroids and steady, axi-symmetric, viscous, incompressible fluid is flowing through a membrane with uniform velocity $\tilde{\mathbf{U}}(\left|\tilde{\mathbf{U}}\right| = \tilde{U})$ along the positive z axis and the membrane is assumed as stationary. This model can be obtained by taking $\ell \to 0$ in the preceding analysis of Sect. 3.1.

To find the hydrodynamic permeability of a membrane during the flow of the fluid, we used the cell model technique, and hence, we select a porous oblate $\tilde{r} = \tilde{a}(1 + 2\varepsilon G_2(\zeta))$ from the membrane and assume that it is confined by the hypothetical cell $\tilde{r} = \tilde{b}(1 + 2\varepsilon G_2(\zeta))$ with the same geometry as the porous oblate (Fig. 7b). In this case, the stream function formulation of the governing equations for the flow outside the porous region and inside the porous region, respectively, will become:

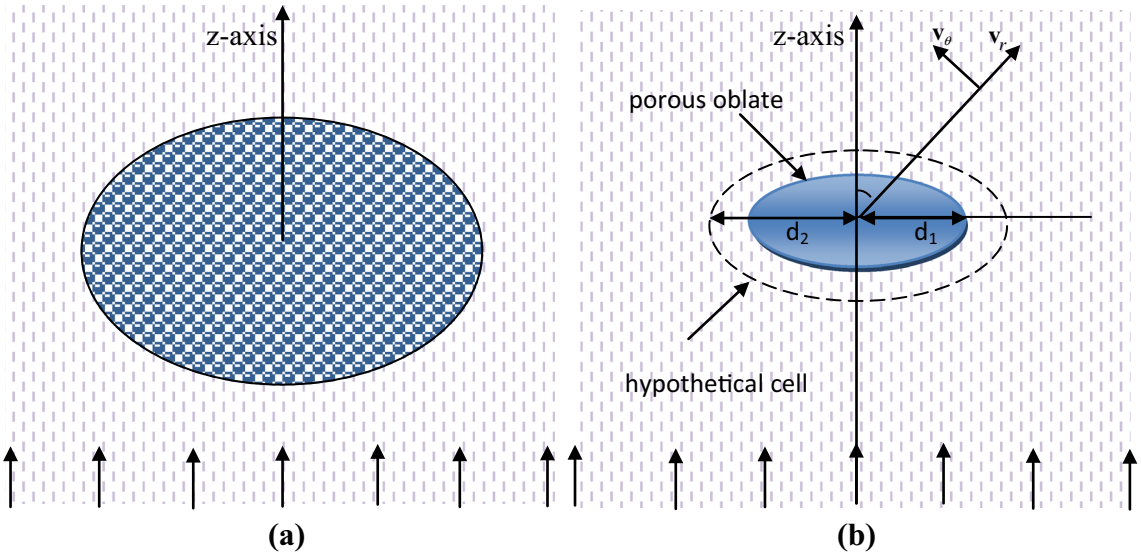

Fig. 7 **a** Membrane built up by porous oblate spheroid. **b** Coordinate system of the problem

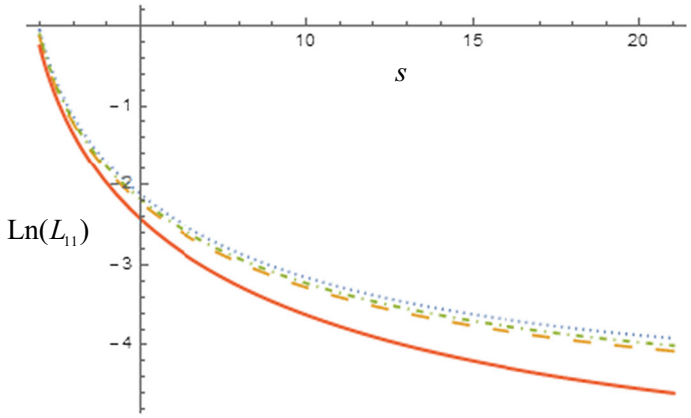

Fig. 8 Variation of natural logarithm of the dimensionless hydrodynamic permeability, L_{11}, of a membrane built up by porous oblate spheroid with parameter s for the all four models at, $\gamma = 0.8$, $\lambda = 1$, $\varepsilon = 0.05$, $k = 0.5$ and $\beta = 0.5$

$$\psi^o = \left[a_2 r^2 + \frac{b_2}{r} + c_2 r + d_2 r^4\right] G_2(\zeta) + \left[A_2 r^2 + B_2 r^{-1} + C_2 r + D_2 r^4\right] G_2(\zeta) + \left[A_4 r^4 + B_4 r^{-3} + C_4 r^{-1} + D_4 r^6\right] G_4(\zeta), \tag{69}$$

$$\psi^i = \left[a_2^* r^2 + d_2^* y_2(sr)\right] G_2(\zeta) + [A_2^* r^2 + D_2^* y_2(sr)] G_2(\zeta) + [A_4^* r^4 + D_4^* y_4(sr)] G_4(\zeta). \tag{70}$$

The arbitrary constants $a_2, b_2, c_2, d_2, A_2, B_2, C_2, D_2, A_4, B_4, C_4, D_4, a_2^*, d_2^*, A_2^*, D_2^*, A_4^*$ and D_4^* can be obtained by using the boundary conditions (28)–(30) on the porous–fluid interface and (31)–(35) on the hypothetical cell with the perturbation method approach. After finding the arbitrary constants, we can obtain the permeability of the membrane with the help of $L_{11} = \frac{1}{3\gamma^3} \frac{(1-\varepsilon)}{\{(1-\varepsilon)c_2 + C_2\}}$.

The effect of various parameters like permeability parameter s, viscosity ratio λ, particle volume fraction γ, deformation parameter ε and stress jump coefficient β on the dimensionless hydrodynamic permeability, L_{11}, of a membrane built up by porous oblate spheroids is shown in Fig. 8, 9, 10, 11 and 12. These figures clearly show the effect of these parameters on the hydrodynamic permeability of the membrane. The nature of the variation in the dimensionless hydrodynamic permeability, L_{11}, of a membrane built up by porous oblate spheroid with different parameters are almost same as in the case of a membrane built up by impermeable oblate spheroids coated with a porous layer. From these figures, it is also observed that the dimensionless hydrody-

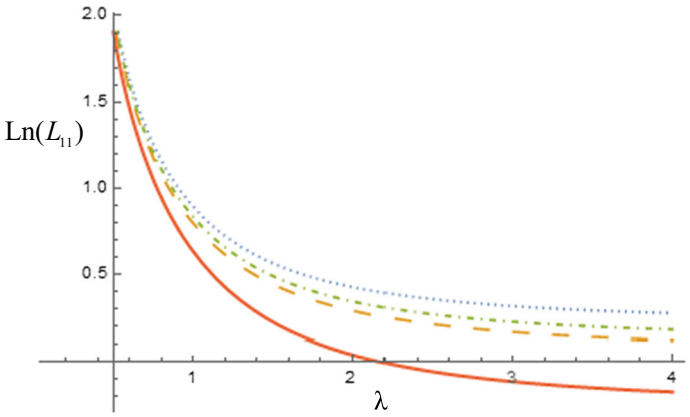

Fig. 9 Variation of natural logarithm of the dimensionless hydrodynamic permeability, L_{11}, of a membrane built up by porous oblate spheroid with parameter λ for all four models at, $\gamma = 0.4$, $s = 5$, $\varepsilon = 0.1$, $k = 0.5$ and $\beta = 0.5$

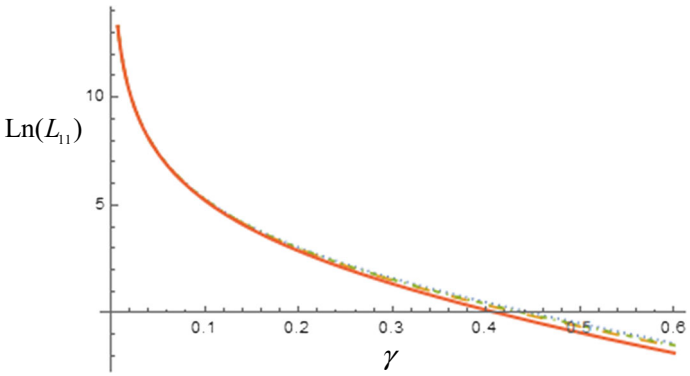

Fig. 10 Dependence of natural logarithm of the dimensionless hydrodynamic permeability, L_{11}, of a membrane built up by porous oblate spheroid with parameter γ for all models at, $\lambda = 2$, $s = 4$, $\varepsilon = 0.1$, $k = 0.5$ and $\beta = 0.5$

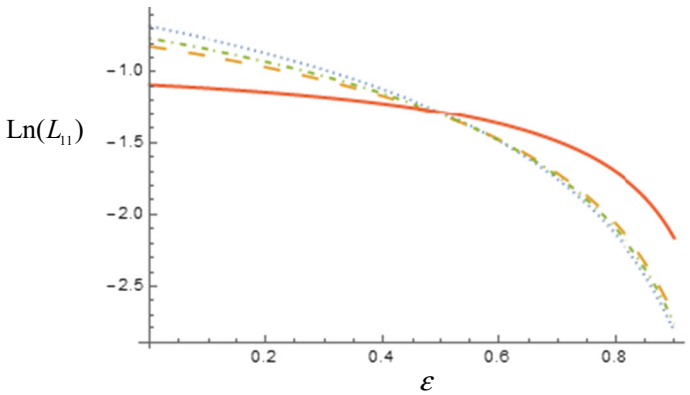

Fig. 11 Variation of natural logarithm of the dimensionless hydrodynamic permeability, L_{11}, of a membrane built up by porous oblate spheroid with parameter ε for all models at, $\lambda = 1$, $s = 5$, $\gamma = 0.6$, $\ell = 0.5$, $k = 0.5$ and $\beta = 0.5$

namic permeability, L_{11}, of a membrane built up by porous oblate spheroids is higher than the hydrodynamic permeability, L_{11}, of a membrane built up by impermeable oblate spheroids coated with a porous layer.

The ratio Ω of drag force $\tilde{F} = 4\pi\tilde{\mu}^o d\tilde{U}[(1-\varepsilon)c_2 + C_2]$ to Stokes force $\tilde{F}_S = 6\pi d\tilde{\mu}^o\tilde{U}$ will be

$$\Omega = \frac{2}{3}[(1-\varepsilon)c_2 + C_2]. \tag{71}$$

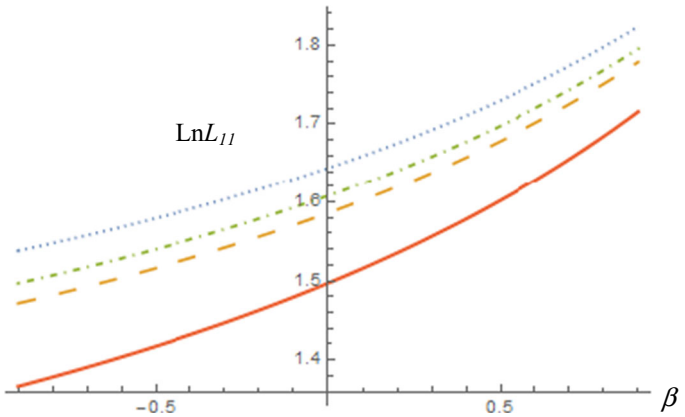

Fig. 12 Variation of natural logarithm of the dimensionless hydrodynamic permeability, L_{11}, of a membrane built up by porous oblate spheroid with the stress jump coefficient β at $\gamma = 0.3$, $\varepsilon = 0.3\, s = 5$, $k = 0.5$ and $\lambda = 1$

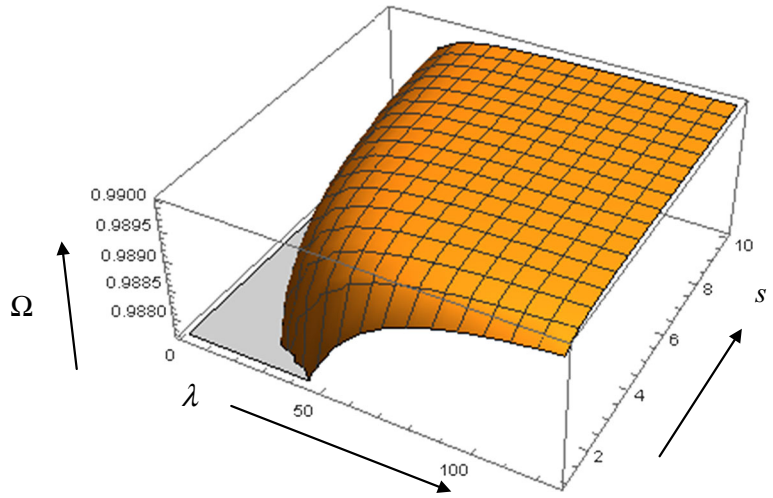

Fig. 13 Variation of Ω with λ and s when $\beta = 0.5$ and $\varepsilon = 0.3$

The effect of viscosity ratio λ and permeability parameter s on the drag force ratio Ω is shown in Fig. 13. From this figure, we obtain that the drag force ratio Ω increases with increasing viscosity ratio λ and permeability parameter s. It is also found that the variation in Ω for higher values of viscosity ratio λ becomes almost constant for a given permeability parameter s. The variation of Ω with deformation parameter ε and permeability parameter s is shown in Fig. 14 with the conclusion that the ratio Ω increases with the permeability parameter s, but it decreases when the deformation parameter ε increases. The effect of viscosity ratio, deformation parameter and stress jump coefficient, permeability parameter on Ω is discussed in Figs. 15 and 16, respectively.

Particular Cases

i. Flow through a membrane composed of a porous oblate spheroid in an unbounded medium

When $\tilde{b} \to \infty$, i.e. $\gamma \to 0$, our present problem will become the porous oblate spheroid in an unbounded medium. In this case, the values of hydrodynamic drag force and drag force ratio (with stokes force) Ω, respectively, become

$$\tilde{F} = 4\pi\tilde{\mu}^o d_1 \tilde{U} X, \tag{72}$$

$$\Omega = \frac{2}{3} X, \tag{73}$$

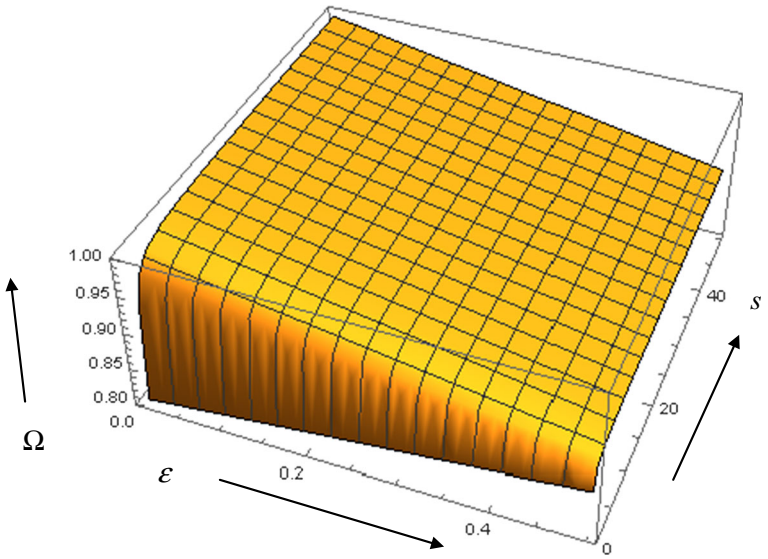

Fig. 14 Variation of Ω with ε and s when $\beta = 0.5$ and $\lambda = 5$

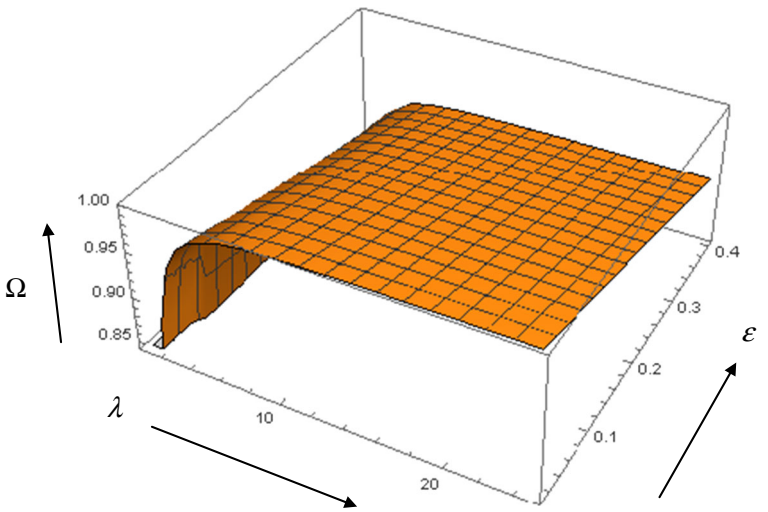

Fig. 15 Variation of Ω with λ and ε when $\beta = 0.5$ and $s = 5$

where

$$
\begin{aligned}
\mathrm{X} = {} & (3(s^2 \mathrm{Sinh}[s]\,((\alpha^2\beta^2(5\left(36+\left(60+s^2\right)\lambda^2-2\left(48-16s^2+s^4\right)\lambda^4\right) \\
& +\epsilon(12-7\left(-12+s^2\right)\lambda^2+2\left(48-16s^2+s^4\right)\lambda^4)) \\
& +2s^2\lambda^2(-5\left(-1+\lambda^2\right)(18+3\left(18+s^2\right)\lambda^2 \\
& +2s^2(6+s^2)\lambda^4)+\epsilon\left(18+3\left(12+53s^2\right)\lambda^2-\left(54+75s^2+10s^4\right)\lambda^4+2s^2\left(6+s^2\right)\lambda^6\right)) \\
& +\alpha\beta(-5(72+48\left(3+s^2\right)\lambda^2+\left(-216+120s^2+7s^4\right)\lambda^4+2s^2(-48+4s^2+s^4)\lambda^6) \\
& +\epsilon(-504+168\left(-6+s^2\right)\lambda^2-3\left(-504+16s^2+13s^4\right)\lambda^4+2s^2(-48+4s^2+s^4)\lambda^6))))\,(s\mathrm{Cosh}[s]-\mathrm{Sinh}[s]) \\
& +s^2(\alpha^2\beta^2(\epsilon(12+\left(20+s^2\right)\lambda^2-2\left(-4+s^2\right)^2\lambda^4)+5\left(36+17\left(-4+s^2\right)\lambda^2+2\left(-4+s^2\right)^2\lambda^4\right)) \\
& +4s^2\lambda^2(5(-1+\lambda^2)\left(-9-3\left(-3+s^2\right)\lambda^2+2s^2\lambda^4\right)+\epsilon\left(9-3\left(6+s^2\right)\lambda^2+\left(9+5s^2+2s^4\right)\lambda^4-2s^2\lambda^6\right))
\end{aligned}
$$

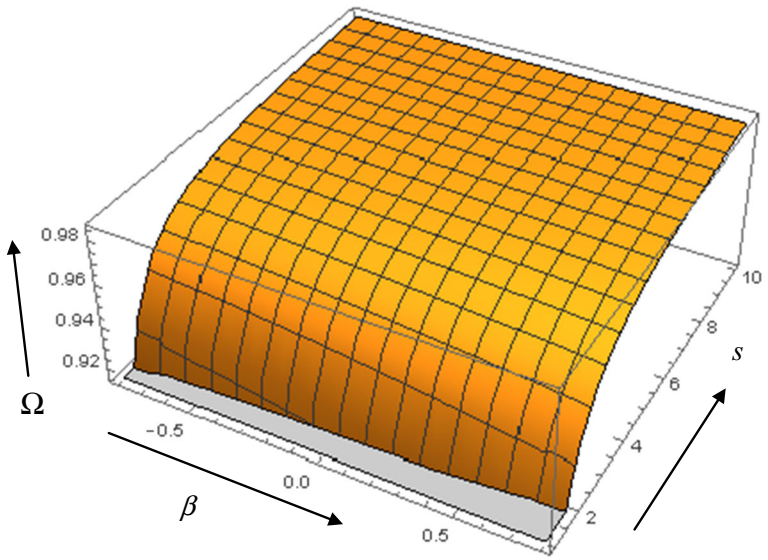

Fig. 16 Variation of Ω with β and s when $\lambda = 5$ and $\varepsilon = 0.5$

$$
\begin{aligned}
&-2\alpha\beta(\epsilon\left(252+18\left(-28+3s^2\right)\lambda^2+\left(252-38s^2-9s^4\right)\lambda^4+4s^2\left(-4+s^2\right)\lambda^6\right)\\
&-5(-36+\left(72-30s^2\right)\lambda^2+\left(-36+46s^2-5s^4\right)\lambda^4+4s^2(-4+s^2)\lambda^6)))\text{Sinh}\,[s])\\
&-\left(s\text{Cosh}\,[s]-\text{Sinh}\,[s]\right)((\alpha^2\beta^2(5(108-15\left(-12+s^2\right)\lambda^2\\
&-2\left(-12+s^2\right)^2\lambda^4)+\epsilon\left(36+\left(252+33s^2-8s^4\right)\lambda^2+2\left(-12+s^2\right)^2\lambda^4\right))\\
&+s^2\lambda^2(-5\left(-108-216\lambda^2-9\left(-36+s^4\right)\lambda^4+2s^2\left(6+s^2\right)^2\lambda^6\right)+\epsilon(108+24(9+36s^2+4s^4)\lambda^2\\
&+\left(-324-720s^2-63s^4+8s^6\right)\lambda^4+2s^2\left(6+s^2\right)^2\lambda^6))\\
&+2\alpha\beta(-5(108+54\left(4+s^2\right)\lambda^2+3\left(-108+42s^2+s^4\right)\lambda^4+2s^2\left(-72-6s^2+s^4\right)\lambda^6)+\epsilon(-756+6(-252+57s^2\\
&+8s^4)\lambda^2-3\left(-756-66s^2+5s^4\right)\lambda^4+2s^2\left(-72-6s^2+s^4\right)\lambda^6)))(s\text{Cosh}\,[s]-\text{Sinh}\,[s])\\
&+s^2(\alpha^2\beta^2(\epsilon\left(36+\left(60-7s^2\right)\lambda^2-2\left(48-16s^2+s^4\right)\lambda^4\right)\\
&+5(108+3\left(-68+11s^2\right)\lambda^2+2\left(48-16s^2+s^4\right)\lambda^4))-2s^2\lambda^2(-5(54+9\left(-12+s^2\right)\lambda^2\\
&-3\left(-18+7s^2+s^4\right)\lambda^4+2s^2\left(6+s^2\right)\lambda^6)+\epsilon(-54+9\left(12+7s^2\right)\lambda^2\\
&-(54+75s^2+7s^4)\lambda^4+2s^2\left(6+s^2\right)\lambda^6))-\alpha\beta(\epsilon(1512+144\left(-21+s^2\right)\lambda^2\\
&+(1512-48s^2-43s^4)\lambda^4+2s^2\left(-48+4s^2+s^4\right)\lambda^6)-5(-216-144\left(-3+s^2\right)\lambda^2\\
&-3\left(72-80s^2+3s^4\right)\lambda^4+2s^2\left(-48+4s^2+s^4\right)\lambda^6)))\text{Sinh}\,[s])))/(5((-18-3\left(18+s^2\right)\lambda^2-2s^2(6+s^2)\lambda^4\\
&+\alpha\beta\left(9-2\left(-12+s^2\right)\lambda^2\right))\left(s\text{Cosh}\,[s]-\text{Sinh}\,[s]\right)+s^2(\alpha\beta(9+2(-4+s^2)\lambda^2)\\
&+2\left(-9-3\left(-3+s^2\right)\lambda^2+2s^2\lambda^4\right))\text{Sinh}\,[s])(-(-54-9\left(-6+s^2\right)\lambda^2\\
&+2s^2\left(6+s^2\right)\lambda^4+\alpha\beta\left(27+2\left(-12+s^2\right)\lambda^2\right))\left(s\text{Cosh}\,[s]-\text{Sinh}\,[s]\right)+s^2(\alpha\beta(9+2\left(-4+s^2\right)\lambda^2)\\
&+2\left(-9-3\left(-3+s^2\right)\lambda^2+2s^2\lambda^4\right))\text{Sinh}\,[s]))
\end{aligned}
$$

ii. Flow through solid oblate spheroid in a cell

Under the limiting case $s \to \infty$, the considered physical problems will reduce to the problem of flow through the solid oblate spheroid in a cell. In this case, the values of dimensionless hydrodynamic permeability for all the models become:

Happel's model:

$$L_{11} = -\frac{5(-1+\gamma)^4(1+\gamma)^2(2+\gamma+2\gamma^2)^2(-1+\epsilon)}{3\gamma^3(3+2\gamma^5)(-5(-2-\gamma+\gamma^3+2\gamma^4)+(-2+\gamma(5+3\gamma(4+\gamma(3+2\gamma))))\epsilon)}. \tag{74}$$

Kuwabara's model:

$$L_{11} = -\frac{2(-1+\gamma)^4(5+\gamma(6+\gamma(3+\gamma)))^2(-1+\epsilon)}{9\gamma^3(-5(-1+\gamma)(5+\gamma(6+\gamma(3+\gamma)))+(-5+\gamma(8+7\gamma(3+\gamma(2+\gamma))))\epsilon)}. \tag{75}$$

Kvashnin's model:

$$L_{11} = -\frac{5(-1+\gamma)^4(16+\gamma(21+\gamma(15+8\gamma)))^2(-1+\epsilon)}{18\gamma^3(4+\gamma^5)(-5\gamma(-5+\gamma(6+\gamma(7+8\gamma)))-16(-5+\epsilon)+\gamma(31+\gamma(78+\gamma(55+32\gamma)))\epsilon)}. \tag{76}$$

Mehta–Morse's model:

$$L_{11} = -\frac{5(-1+\gamma)^3(4+\gamma(7+4\gamma))(-1+\varepsilon)}{18\gamma^3(1+\gamma+\gamma^2+\gamma^3+\gamma^4)(-5+\varepsilon)}. \tag{77}$$

These results agree with the previously established results of Yadav et al. [32].

iii. Flow through solid oblate spheroid in an unbounded medium

When $\tilde{b} \to \infty$, i.e. $\gamma \to 0$ and $s \to \infty$, then the physical problem will reduce to the flow through a solid oblate spheroid in an unbounded medium, and in this case, the drag force exerted on the solid oblate spheroid by the flow of fluid and the drag force ratio (with Stokes force) Ω, respectively, are given as

$$\tilde{F} = 6\pi\tilde{\mu}^o d_1 \tilde{U}\left(1-\frac{\varepsilon}{5}\right), \tag{78}$$

$$\Omega = 1-\frac{\varepsilon}{5}. \tag{79}$$

The result (78) for the drag force experienced by a solid oblate spheroid in an unbounded medium agrees with the result of Palaniappan [21], Ramkissoon [25] and Datta and Deo [27] for the flow past a rigid spheroid in an unbounded medium.

iv. Flow through porous sphere in cell

When $\varepsilon \to 0$, then the model discussed in Sect. 3.2 will reduce to the flow of steady, viscous, incompressible fluid through a swarm of porous spherical particles, and in this case, the expression for the dimensionless hydrodynamic permeability of the membrane built up by porous spherical particles for all models will be as follows:

Happel's model:

$$\begin{aligned}
\mathrm{L}_{11} = {} & (s(54(-1+\gamma^5)+3(18+12\gamma^5+s^2(-3+6\gamma+8\gamma^5-6\gamma^6))\lambda^2 \\
& -s^2(6+s^2)(-1+\gamma)^3(1+\gamma)(2+\gamma+2\gamma^2)\lambda^4+\alpha\beta(9(3-4\gamma+2\gamma^5+4\gamma^6) \\
& -(-12+s^2)(-1+\gamma)^3(1+\gamma)(2+\gamma+2\gamma^2)\lambda^2))\mathrm{Cosh}[s] \\
& +(-3(3+s^2)(-6+6\gamma^5+\alpha\beta(3-4\gamma+2\gamma^5 \\
& +4\gamma^6))+(-3s^2(3+6\gamma-6(-2+\gamma)\gamma^5+\alpha\beta(-2+3\gamma-3\gamma^5+2\gamma^6))+s^4(6-6\gamma \\
& +6(-1+\gamma)\gamma^5+\alpha\beta(-2+3\gamma-3\gamma^5+2\gamma^6))-6(9+6\gamma^5+2\alpha\beta(-2+3\gamma \\
& -3\gamma^5+2\gamma^6)))\lambda^2+3s^2(2+s^2)(-1+\gamma)^3(1+\gamma)(2+\gamma \\
& +2\gamma^2)\lambda^4)\mathrm{Sinh}[s])/(3\gamma^3(s(\alpha\beta(-36(-1+\gamma^5)+(-12+s^2)(3+2\gamma^5)\lambda^2) \\
& +s^2\lambda^2(18(-1+\gamma^5)+(6+s^2)(3+2\gamma^5)\lambda^2))\mathrm{Cosh}[s]-(3s^2\lambda^2(2(3+s^2)(-1+\gamma^5) \\
& +(2+s^2)(3+2\gamma^5)\lambda^2) \\
& +\alpha\beta(-12(3+s^2)(-1+\gamma^5) \\
& +(-12-3s^2+s^4)(3+2\gamma^5)\lambda^2))\mathrm{Sinh}[s]))
\end{aligned} \tag{80}$$

Kuwabara's model:

$$\begin{aligned}L_{11} = {} & (s(-270 - 9(-30 + s^2(5 + 2\gamma(-6 + \gamma^5)))\lambda^2 - 2s^2(6 + s^2)(-1 + \gamma)^3(5 + \gamma(6 + \gamma(3 \\ & + \gamma)))\lambda^4 + \alpha\beta(9(15 + 4\gamma(-6 + 5\gamma^2 + \gamma^5)) - 2(-12 + s^2)(-1 + \gamma)^3(5 + \gamma(6 \\ & + \gamma(3 + \gamma)))\lambda^2))\text{Cosh}[s] + (-3(3 + s^2)(-30 + \alpha\beta(15 + 4\gamma(-6 + 5\gamma^2 + \gamma^5))) \\ & + (2s^4(3(5 - 6\gamma + \gamma^6) + \alpha\beta(-5 + 9\gamma - 5\gamma^3 + \gamma^6)) - 3s^2(15 + 36\gamma - 6\gamma^6 \\ & + 2\alpha\beta(-5 + 9\gamma - 5\gamma^3 + \gamma^6)) - 6(45 + 4\alpha\beta(-5 + 9\gamma - 5\gamma^3 + \gamma^6)))\lambda^2 + 6s^2(2 \\ & + s^2)(-1 + \gamma)^3(5 + \gamma(6 + \gamma(3 + \gamma)))\lambda^4)\text{Sinh}[s])/(45\gamma^3(s(\alpha\beta(12 + (-12 + s^2)\lambda^2) \\ & + s^2\lambda^2(-6 + (6 + s^2)\lambda^2))\text{Cosh}[s] - (s^2\lambda^2(-2(3 + s^2) + 3(2 + s^2)\lambda^2) \\ & + \alpha\beta(4(3 + s^2) + (-12 - 3s^2 + s^4)\lambda^2))\text{Sinh}[s])) \end{aligned} \tag{81}$$

Kvashnin's model:

$$\begin{aligned}L_{11} = {} & (s(54(-8 + 3\gamma^5) - 18(-6(4 + \gamma^5) + s^2(4 + \gamma(-9 + 4(-1 + \gamma)\gamma^4)))\lambda^2 - s^2(6 \\ & + s^2)(-1 + \gamma)^3(16 + \gamma(21 + \gamma(15 + 8\gamma)))\lambda^4 + \alpha\beta(18(12 - 18\gamma + 10\gamma^3 + 3\gamma^5 \\ & + 8\gamma^6) - (-12 + s^2)(-1 + \gamma)^3(16 + \gamma(21 + \gamma(15 + 8\gamma)))\lambda^2))\text{Cosh}[s] \\ & + (-6(3 + s^2)(-24 + 9\gamma^5 + \alpha\beta(12 - 18\gamma + 10\gamma^3 + 3\gamma^5 + 8\gamma^6)) + (s^4(48 - 54\gamma \\ & + 6\gamma^5(-3 + 4\gamma) + \alpha\beta(-1 + \gamma)^3(16 + \gamma(21 + \gamma(15 + 8\gamma)))) \\ & - 12(9(4 + \gamma^5) + \alpha\beta(-1 + \gamma)^3(16 + \gamma(21 + \gamma(15 + 8\gamma)))) \\ & - 3s^2(6(4 + 9\gamma + 6\gamma^5 - 4\gamma^6) + \alpha\beta(-1 + \gamma)^3(16 + \gamma(21 + \gamma(15 + 8\gamma))))\lambda^2 \\ & + 3s^2(2 + s^2)(-1 + \gamma)^3(16 + \gamma(21 + \gamma(15 + 8\gamma)))\lambda^4)\text{Sinh}[s])/(18\gamma^3(s(\alpha\beta(48 - 18\gamma^5 \\ & + (-12 + s^2)(4 + \gamma^5)\lambda^2) + s^2\lambda^2(-24 + 9\gamma^5 + (6 + s^2)(4 + \gamma^5)\lambda^2))\text{Cosh}[s] \\ & - (s^2\lambda^2((3 + s^2)(-8 + 3\gamma^5) + 3(2 + s^2)(4 + \gamma^5)\lambda^2) \\ & + \alpha\beta(-2(3 + s^2)(-8 + 3\gamma^5) + (-12 - 3s^2 \\ & + s^4)(4 + \gamma^5)\lambda^2))\text{Sinh}[s])) \end{aligned} \tag{82}$$

Mehta–Morse's model:

$$\begin{aligned}L_{11} = {} & (s(54(2 + 3\gamma^5) - 18(6 - 6\gamma^5 + s^2(-1 + \gamma(3 + 2(-2 + \gamma)\gamma^4)))\lambda^2 - s^2(6 \\ & + s^2)(-1 + \gamma)^4(4 + \gamma(7 + 4\gamma))\lambda^4 + \alpha\beta(18(-3 + 6\gamma - 10\gamma^3 + 3\gamma^5 + 4\gamma^6) \\ & - (-12 + s^2)(-1 + \gamma)^4(4 + \gamma(7 + 4\gamma))\lambda^2))\text{Cosh}[s] + (-6(3 + s^2)(6 + 9\gamma^5 \\ & + \alpha\beta(-3 + 6\gamma - 10\gamma^3 + 3\gamma^5 + 4\gamma^6)) + (s^4(-1 + \gamma)^3(6(1 + \gamma)(2 + \gamma + 2\gamma^2) \\ & + \alpha\beta(-1 + \gamma)(4 + \gamma(7 + 4\gamma))) - 12(-9 + 9\gamma^5 + \alpha\beta(-1 + \gamma)^4(4 + \gamma(7 + 4\gamma))) \\ & - 3s^2(\alpha\beta(-1 + \gamma)^4(4 + \gamma(7 + 4\gamma)) - 6(1 + \gamma(3 + 2(-3 + \gamma)\gamma^4))))\lambda^2 + 3s^2(2 \\ & + s^2)(-1 + \gamma)^4(4 + \gamma(7 + 4\gamma))\lambda^4)\text{Sinh}[s])/(18\gamma^3(s(\alpha\beta(-6(2 + 3\gamma^5) + (-12 \\ & + s^2)(-1 + \gamma^5)\lambda^2) + s^2\lambda^2(6 + 9\gamma^5 + (6 + s^2)(-1 + \gamma^5)\lambda^2))\text{Cosh}[s] \\ & + (s^2\lambda^2(-(3 + s^2)(2 + 3\gamma^5) - 3(2 + s^2)(-1 + \gamma^5)\lambda^2) + \alpha\beta(2(3 + s^2)(2 + 3\gamma^5) \\ & - (-12 - 3s^2 + s^4)(-1 + \gamma^5)\lambda^2))\text{Sinh}[s])) \end{aligned} \tag{83}$$

These results agree with the result of Yadav et al. [12].

v. Flow through porous sphere in an unbounded medium

When $\tilde{b} \to \infty$, i.e. $\gamma \to 0$, $\varepsilon = 0$, then model discussed in Sect. 3.2 will reduce to the flow through a porous sphere in an unbounded medium. In this case, the hydrodynamic drag force experienced by the porous sphere and the drag force ratio (with Stokes force) Ω become:

$$\tilde{F} = \frac{12\pi\tilde{\mu}^o\tilde{U}\tilde{a}\lambda^2 s^2[s(-6+\lambda^2(6+s^2))\cosh s + (-3\lambda^2(2+s^2)+2(3+s^2))\sinh s]}{s(-54+\lambda^2(54+s^2(-9+2\lambda^2(6+s^2))))\cosh s - 3(-6(3+s^2)+\lambda^2(18+(3+4\lambda^2)s^2+2(-1+\lambda^2)s^4))\sinh s},$$

$$\Omega = \left[1 + \frac{9}{2\lambda s^2} + \frac{1}{2(1-\lambda)-\lambda/Q}\right]^{-1},$$

where

$$Q = 1 + \frac{3}{s^2} - \left(1 - \frac{\tanh s}{s}\right)^{-1}.$$

When $\lambda = 1$, then the value of the hydrodynamic drag force exerted by fluid on the porous sphere of radius $\tilde{a}$ will be

$$\tilde{F} = 6\pi\tilde{\mu}^o\tilde{a}\tilde{U}\left[1 + \lambda_2 + \frac{3}{2s^2}\right]^{-1}, \quad \lambda_2 = \sinh s/(s\cosh s - \sinh s),$$

and the dimensionless hydrodynamic drag force ratio Ω

$$\Omega = \left[\left(1 - \frac{\tanh s}{s}\right)^{-1} + \frac{3}{2s^2}\right]^{-1}.$$

These results agree with the previously established results of Vasin and Filippov [37].

vi. Flow through solid sphere in cell

When $s \to \infty$ and $\varepsilon = 0$, then our present problem reduces to fluid flow through a solid sphere in a cell. Here, the dimensionless hydrodynamic permeability of a membrane for all the models is given as:

Happel's model:

$$L_{11} = \frac{-2\gamma^6 + 3\gamma^5 - 3\gamma + 2}{6\gamma^8 + 9\gamma^3},$$

which agrees with the expression in Ref. [7];

Kuwabara's model:

$$L_{11} = \frac{-2(\gamma^6 - 5\gamma^3 + 9\gamma - 5}{45\gamma^3},$$

which agrees with the expression in Ref. [8];

Kvashnin's model:

$$L_{11} = \frac{-(\gamma-1)^3(8\gamma^3 + 15\gamma^2 + 21\gamma + 16}{18\gamma^8 + 72\gamma^3},$$

which agrees with the expression in Ref. [11].

Mehta–Morse's model:

$$L_{11} = \frac{(1-\gamma)^3(4\gamma^2 + 7\gamma + 4)}{18\gamma^3(\gamma^4 + \gamma^3 + \gamma^2 + \gamma + 1)},$$

The above expression for permeability agrees with the expression in Ref. [9];

vii. Flow through solid sphere in an unbounded medium

The flow of viscous, steady, incompressible fluid through a solid sphere in an unbounded medium is the limiting case of the previous section for $\gamma \to 0$.

The drag force F experienced by the solid sphere in an unbounded medium is given as:

$$\tilde{F} = 6\pi\tilde{\mu}^o\tilde{a}\tilde{U}.$$

This is a well-known result for the drag force reported earlier by Stokes [3].

4 Conclusions

Stokes flow past a swarm of oblate spheroidal particles has been studied, and the effect of volume fraction, porosity, permeability parameter, stress jump coefficient on hydrodynamic permeability and drag force (relative to Stokes drag) is analysed. Limiting cases of porous oblate spheroidal particles have been separately investigated, and previously established results of Stokes drag, and drag on porous spheres for all four cell models have been deduced to validate our model.

Acknowledgements The first author is thankful to Science and Engineering Research Board (SERB), New Delhi, Government of India, for supporting this research work under the research Grant SR/ FTP/ MS-47/ 2012.

Compliance with ethical standards

Conflict of interest Dr. Pramod Kumar Yadav has received a research grant from Science and Engineering Research Board, Govt. of India. Dr. Ashish Tiwari and Ms. Priyanka Singh declare that they have no conflict of interest.

References

1. Darcy, H.P.G.: Les fontaines publiques de la ville de Dijon Paris: Victor Dalmont (1856)
2. Brinkman, H.C.: A calculation of viscous force exerted by a flowing fluid on a dense swarm of particles. J. Appl. Sci. Res. **A1**, 27–36 (1947)
3. Stokes, G.G.: On the effects of internal friction of fluids on pendulums. J. Trans. Cambr. Philos. Soc. **9**, 8–106 (1851)
4. Veerapaneni, S., Wiesner, M.R.: Hydrodynamics of fractal aggregates with radially varying permeability. J Colloid Interface Sci. **177**(1), 45–57 (1996)
5. Uchida, S.: Viscous flow in multiparticle systems: slow viscous flow through a mass of particles. Int. Sci. Technol. Univ. Tokyo **3**, 97 (1949). (in Japanese) (Abstract, Ind. Engng. Chem. **46**, 1194–1195 (translated by T. Motai) (1954))
6. Happel, J.: Viscous flow in multiparticle system: slow motion of fluids relative to beds of spherical particles. A. I. Ch. E. **4**(2), 197–201 (1958)
7. Happel, J.: Viscous flow relative to arrays of cylinders. A. I. Ch. E. **5**(2), 174–177 (1959)
8. Kuwabara, S.: The forces experienced by randomly distributed parallel circular cylinders or spheres in a viscous flow at small Reynolds number. J. Phys. Soc. Jpn. **14**, 527–532 (1959)
9. Mehta, G.D., Morse, T.F.: Flow through charged membranes. J. Chem. Phys. **63**(5), 1878–1889 (1975)
10. Cunningham, E.: On the steady state fall of spherical particles through fluid medium. Proc. R. Soc. Lond. A **83**, 357–365 (1910)
11. Kvashnin, A.G.: Cell model of suspension of spherical particles. Fluid Dyn. **14**, 598–602 (1979)
12. Yadav, P.K., Tiwari, A., Deo, S., Filippov, A.N., Vasin, S.: Hydrodynamic permeability of membranes built up by spherical particles covered by porous shells: effect of stress jump condition. Acta Mech. **215**, 193–209 (2010)
13. Deo, S., Filippov, A.N., Tiwari, A., Vasin, S.I., Starov, V.: Hydrodynamic permeability of aggregates of porous particles with an impermeable core. Adv. Coll. Interface Sci. **164**(1), 21–37 (2011)
14. Happel, J., Brenner, H.: Low Reynolds Number hydrodynamics. Martinus Nijoff Publishers, The Hague (1983)
15. Oberbeck, A., Stationare, U.: Fliissigkeitsbewegungen mit Berucksichtigung der inneren Reibung. J. Reine Angew. Math. **81**, 62–80 (1876)
16. Sampson, R.A.: On Stoke's current function. Philos. Trans. R. Soc. Lond. Ser. A **182**, 449–518 (1891)
17. Payne, L.E., Pell, W.H.: The Stokes flow problem for a class of axially symmetric bodies. J. Fluid. Mech. **7**, 529–549 (1960)
18. Acrivos, A., Taylor, T.D.: The Stokes flow past an arbitrary particle: the slightly deformed sphere. Chem. Eng. Sci. **19**, 445–451 (1964)
19. Epstein, N., Masliyah, J.H.: Creeping flow through clusters of spheroids and elliptical cylinders. Chem. Eng. J. **3**, 169–175 (1972)
20. Ramkissoon, H.: Stokes flow past a slightly deformed fluid sphere. Z.A.M.P **37**, 859–866 (1986)
21. Palaniappan, D.: Creeping flow about a slightly deformed sphere. Z. Angew. Math. Phys. **45**, 832–838 (1994)
22. Dassios, G., Hadjinicolaou, M., Payatakes, A.C.: Generalized Eigen function and complete semi separable solutions for Stokes flow in spheroidal coordinates. Q. Appl. Math. **52**, 157–191 (1994)
23. Dassios, G., Hadjinicolaou, M., Coutelieris, F.A., Payatakes, A.C.: Stokes flow in spheroidal particle-in-cell models with Happel and Kuwabara boundary conditions. Int. J. Eng. Sci. **33**(10), 1465–1490 (1995)
24. Burganos, V.N., Coutelieris, F.A., Dassios, G., Payatakes, A.C.: On the rapid convergence of the analytical solution of Stokes flow around spheroids-in-cell. Chem. Eng. Sci. **50**(20), 3313–3317 (1995)
25. Ramkissoon, H.: Slip flow past an approximate spheroid. Acta Mech. **123**, 227–233 (1997)
26. Zlatanovski, T.: Axi-symmetric creeping flow past a porous prolate spheroidal particle using the Brinkman model. Q. J. Mech. Appl. Math. **52**(1), 111–126 (1999)
27. Datta, S., Deo, S.: Stokes flow with slip and Kuwabara boundary conditions. Proc. Indian Acad. Sci. (Math. Sci.) **112**(3), 463–475 (2002)
28. Srinivasacharya, D.: Creeping flow past a porous approximate sphere. Z. Angew Math. Mech. **83**(7), 1–6 (2003)
29. Deo, S.: Stokes flow past a swarm of deformed porous spheroidal particles with Happel boundary condition. J. Porous Media **12**(4), 347–359 (2009)
30. Deo, S., Gupta, B.: Drag on a porous sphere embedded in another porous medium. J. Porous Media **13**(11), 1009–1016 (2010)

31. Yadav, P.K., Deo, S.: Stokes flow past a porous spheroid embedded in another porous medium. Meccanica **47**, 1499–1516 (2012)
32. Yadav, P.K., Deo, S., Yadav, M.K., Filippov, A.N.: On hydrodynamic permeability of a membrane built up by porous deformed spheroidal particles. Colloid J. **75**(5), 611–622 (2013)
33. Langlois, W.E.: Slow Viscous Flow. Macmillan, New York (1964)
34. Abramowitz, M., Stegun, I.A.: Handbook of Mathematical Functions. Dover Publications, New York (1970)
35. Ochoa-Tapia, J.A., Whitaker, S.: Momentum transfer at the boundary between a porous medium and a heterogeneous fluid-I, theoretical development. Int. J. Heat Mass Transf. **38**, 2635–2646 (1995a)
36. Ochoa-Tapia, J.A., Whitaker, S.: Momentum transfer at the boundary between a porous medium and a heterogeneous fluid-II, theoretical development. Int. J. Heat Mass Transf. **38**, 2647–2655 (1995b)
37. Vasin, S.I., Filippov, A.N.: Permeability of complex porous media. Colloid J. **71**(1), 31–45 (2009)